Journal Pre-proof

Looking at the modern landscape of submediterranean Greece through a palaeoecological lens

César Morales-Molino, Lieveke van Vugt, Jacqueline F.N. van Leeuwen, Erika Gobet, Christoph Schwörer, Kathrin Ganz, Tryfon Giagkoulis, Sandra O. Brugger, Amy Bogaard, Albert Hafner, Kostas Kotsakis, André F. Lotter, Willy Tinner

PII: S0048-9697(24)05136-2

DOI: https://doi.org/10.1016/j.scitotenv.2024.174986

Reference: STOTEN 174986

To appear in: *Science of the Total Environment*

Received date: 19 March 2024

Revised date: 20 July 2024

Accepted date: 21 July 2024

Please cite this article as: C. Morales-Molino, L. van Vugt, J.F.N. van Leeuwen, et al., Looking at the modern landscape of submediterranean Greece through a palaeoecological lens, *Science of the Total Environment* (2024), https://doi.org/10.1016/j.scitotenv.2024.174986

Looking at the modern landscape of submediterranean Greece through a palaeoecological lens

César Morales-Molino[a,b,c,*], Lieveke van Vugt[b,c,1], Jacqueline F.N. van Leeuwen[b,c,1], Erika Gobet[b,c], Christoph Schwörer[b,c], Kathrin Ganz[b,c], Tryfon Giagkoulis[d], Sandra O. Brugger[b,c,e,f], Amy Bogaard[g], Albert Hafner[c,h], Kostas Kotsakis[d], André F. Lotter[b,c], Willy Tinner[b,c]

[a] Grupo de Ecología y Restauración Forestal (FORECO), Departamento de Ciencias de la Vida, Facultad de Ciencias, Universidad de Alcalá, Alcalá de Henares, Spain

[b] Institute of Plant Sciences, University of Bern, Bern, Switzerland

[c] Oeschger Centre for Climate Change Research, University of Bern, Bern, Switzerland

[d] School of History and Archaeology, Aristotle University of Thessaloniki, Thessaloniki, Greece

[e] Geoecology, Department of Environmental Sciences, University of Basel, Basel, Switzerland

[f] Analytical Chemistry Laboratory, Paul Scherrer Institute, Villigen, Switzerland

[g] School of Archaeology, University of Oxford, Oxford, United Kingdom

[h] Institute of Archaeological Sciences, University of Bern, Bern, Switzerland

* Corresponding author: cesar.morales@uah.es

[1] L.v.V and J.F.N.v.L. contributed equally to this study.

Abstract

The importance of understanding the long-lasting legacy of past land use on modern ecosystems has long been acknowledged. However, the magnitude and persistence of such legacies have been assessed only occasionally. Northern Greece has been a gateway of farming into mainland Europe during the Neolithic, thus providing a perfect setting to assess the potential impact of land-use history on present-day ecosystems. Additionally, the particularly marked Holocene climatic variability of the southern Balkans makes it possible to investigate climate-vegetation-land use interactions over long timescales. Here, we have studied a sediment record from Limni Vegoritis (Northern Greece) spanning the past ~9000 years using palaeoecological proxies (pollen, spores, stomata, microscopic charcoal). We aimed to reconstruct long-term vegetation dynamics in submediterranean Greece, to assess the environmental factors controlling them and to establish the legacies of the long history of land use in the modern landscape. We found that the Early Holocene afforestation, mainly oak woodlands, was delayed because of suboptimal moisture conditions. Later, colder and drier conditions during the rapid climate change centred around the '8.2 ka event' triggered woodland opening and the spread of wooded (*Juniperus*) steppe vegetation. First indicators of farming activities are recorded during this period, but their abundances are too low to explain the concurrent large deforestation episode. Later, pinewoods (probably dominated by *Pinus nigra*) with deciduous *Quercus* spread and dominated the landscape for several millennia. These forests experienced repeated multi-centennial setback-recovery episodes associated with land-use intensification, but pines eventually declined ~2500—2000 years ago during Classical times under heavy land use comprising intense pastoralism. This was the starting point for the present-day landscape, where the main 'foundation' taxon of the ancient forests (*Pinus* cf. *nigra*) is missing, therefore attesting to the strong imprint that historical land use has left on the modern landscape.

Keywords:

fire history; Holocene; land-use history; Mediterranean region; pastoralism; pollen analysis

1. Introduction

The strong legacy of past land use on modern ecosystem composition, structure and functioning across biomes has been stressed by ecologists and palaeoecologists for the past decades (Foster et al., 2003; McWethy et al., 2010; Perring et al., 2016; Maezumi et al., 2018). Land-use history also seems to condition the response of plant communities to ongoing climate change (Perring et al., 2016; Vilà-Cabrera et al., 2023). Many studies about the legacy of land-use history on modern ecosystems have focused on multi-decadal to centennial timescales (e.g. Foster et al., 2003; Perring et al., 2016; Sánchez de Dios et al., 2021), but palaeoecology has revealed that the imprint of anthropogenic disturbance on ecosystems may have lasted for several centuries or even millennia (Feurdean et al., 2009; Tinner et al., 2013; Whitlock et al., 2018; Cagliero et al., 2022). Historical ecology and, more specifically, palaeoecology thus represent ideal tools to assess the degree to which ecosystems have been disturbed by human activities and the level of naturalness of today's landscapes, as well as to provide guidance to nature restoration and management practitioners (Swetnam et al., 1999; Whitlock et al., 2018; Morales-Molino et al., 2019). In this context, Northern Greece constitutes a perfect arena to evaluate the impact of land-use history on the landscape over long timescales because it was a gateway of farming into Europe during the Neolithic (Roberts et al., 2011; Betti et al., 2020). Additionally, the southern Balkans have experienced remarkable shifts in temperature and precipitation during the Holocene (Rohling and Pälike, 2005; Gogou et al., 2007; Marino et al., 2009; Francke et al., 2013), thus offering the opportunity to explore the responses of vegetation and human societies to climate variability.

Although the southern Balkans have been intensively investigated from a palynological perspective, most published studies have focused on long lake-sediment records usually spanning several tens of thousands of years (e.g. Tzedakis, 1993; Tzedakis et al., 2006; Fletcher et al., 2013; Panagiotopoulos et al., 2014; Milner et al., 2016; Donders et al., 2021) and some mountainous areas (e.g. Stefanova and Ammann, 2003; Stefanova et al., 2006;

Gerasimidis et al., 2009; Gerasimidis and Panajiotidis, 2010; Feurdean et al., 2019; Tonkov, 2021). However, detailed studies on the Lateglacial and the Holocene from sites located at low-to-mid elevations are quite rare (see Fig. 1 and references therein). The number of publications comprehensively discussing postglacial palaeoecological records with a robust chronology is even lower (e.g. Glais et al., 2016, 2017; Gassner et al., 2020; Brechbühl et al., 2024). The location of the mid-elevation Limni Vegoritis in Northern Greece (Fig. 1) where agriculture was introduced in mainland Europe from south-western Asia during the Neolithic (Hofmanová et al., 2016; Betti et al., 2020; Maniatis and Adaktylou, 2021) makes it highly suitable to investigate the legacy of changing land use on the submediterranean landscapes of south-eastern Europe. Already some 40 years ago, Bottema (1982) published a pollen record from this lake that showed the potential of this site to address such research questions. Since then, palaeoecological research tools have developed markedly, enabling significant improvements in the knowledge about long-term landscape dynamics. In our study, we have incorporated several of those developments to enhance the quality of the record, namely: (i) increased time resolution (more samples), (ii) a robust chronology based on a much higher number of radiocarbon dates on short-lived terrestrial plant macrofossils, and (iii) the study of microscopic charcoal particles, as a proxy for extra-local to regional fire occurrence (Tinner et al., 1998; Adolf et al., 2018), and spores of obligate coprophilous fungi, as a proxy for herbivore densities and pastoralism (Gill et al., 2013; Baker et al., 2016).

In this paper, we present a new well-dated palaeoecological record from Limni Vegoritis with the following aims: (i) to track vegetation dynamics in submediterranean Greece during the past ~9000 years and to discuss the environmental factors influencing them; and (ii) to assess the legacy of the long history of land use of this region on the present-day landscape.

2. Material and Methods

2.1 Study site

Limni Vegoritis (coring location: 40°46'58" N, 21°49'12" E, 519 m a.s.l.; Fig. 1) is one of the largest (surface: 47.2 km^2) and deepest (maximum water depth: 52.6 m) natural lakes in Greece (Doulgeris and Argyroudi, 2019). The natural hydrological catchment of Limni Vegoritis extends over 1853 km^2 in Northern Greece (Skoulikidis et al., 1998). However, Limni Zazari, Limni Chimaditis, Limni Petron and Limni Vegoritis were connected by artificial channels during the 20th century CE, which enlarged Limni Vegoritis' catchment to 2145 km^2 (Doulgeris and Argyroudi, 2019). The hydrological catchment is delimited by the Voras Mountains to the north and the Vermio Mountains to the east, both featuring peaks ~2000 m a.s.l. in the catchment. Limni Vegoritis currently has two main inlets: the Pentavryso stream and the excess surface water of Limni Petron, which flows into Limni Vegoritis through a subterranean channel (Doulgeris and Argyroudi, 2019). There is no surface outlet but rather karstic sinkholes. Limni Vegoritis presents two distinct subbasins: the main one, large and deep, and a smaller and shallower one located on the northeastern corner of the lake next to the town of Arnissa (Fig. 1).

The climate in the lowlands around Limni Vegoritis is mainly submediterranean subcontinental (Cfa in the Köppen-Geiger climate classification), whereas the mountains bordering the catchment feature Dfb and Dsb climates characterised by higher precipitation and lower temperatures (Hellenic National Meteorological Service). Mean annual precipitation amounts to ~570 mm at the Arnissa meteorological station, while $P_{July\text{-}September}$ is ~100 mm. At the Florina meteorological station (619 m a.s.l., ~35 km away from the coring site), mean annual temperature is 12.2°C, with $T_{January}$ and T_{July} of 0.6°C and 23.4°C, respectively. Although the geology of the catchment is rather complex and the lithology is variable, carbonate bedrock dominates over broad areas (Pirini et al., 2014).

Below, we briefly describe the main vegetation types in the Limni Vegoritis catchment according to Bohn et al. (2000/2003), Pirini et al. (2014) and our own vegetation surveys in the region (partly published in Senn et al., 2022). In the lowlands surrounding the lake, the vegetation cover mainly consists of herbaceous crops (e.g. cereal fields), fruit tree orchards

(mostly Rosaceae), *'shibljak'* (deciduous thorny scrub typical of submediterranean areas of the Balkan Peninsula), steppe-like grasslands and small degraded deciduous oak woodlands. In the hilly landscape that borders most of the lake and the foothills of the adjacent mountains, open deciduous oak woodlands occur (*Quercus trojana*, *Q. pubescens*, *Q. frainetto*), with an understory rich in deciduous (*Acer monspessulanum*, *Carpinus orientalis*, *Colutea arborescens*, *Paliurus spina-christi*) and evergreen (*Juniperus oxycedrus*, *Phillyrea latifolia*, *Jasminum fruticans*) trees and shrubs. The *'shibljak'* deciduous shrublands (*Paliurus spina-christi*, *Pistacia terebinthus*, *Pyrus spinosa*, *Rhamnus saxatilis*) are widespread throughout, often replacing oak woods. The rocky calcareous hills that separate Limni Vegoritis and Limni Petron are mainly covered with a parkland vegetation consisting of steppe-like grasslands with scattered *Juniperus oxycedrus* and *Quercus trojana*. Higher up (>1000 m a.s.l.), oromediterranean *Fagus sylvatica* forests, often mixed with *Abies borisii-regis* and *Acer pseudoplatanus*, form the dominant vegetation. Towards the timberline (>1650 m a.s.l.), altimediterranean *Pinus sylvestris* forests replace beech stands. At the treeline ecotone (~1900—2000 m a.s.l.), we find subalpine scrub dominated by *Juniperus communis* var. *saxatilis* (=*J. communis* subsp. *alpina*), *Vaccinium myrtillus*, *Daphne oleoides* and *Erica spiculifolia* (=*Bruckenthalia spiculifolia*) with scattered individuals and small stands of *Pinus sylvestris*.

2.2 Coring, radiocarbon dating and age-depth modelling

In April 2016, we collected two surface cores (VEG16-A and VEG16-B) using a UWITEC gravity corer and two overlapping parallel long cores (VEG16-1 and VEG16-2) with a UWITEC piston corer from the deepest part (water depth: 18.5 m) of the smaller Limni Vegoritis subbasin (~290 ha; Fig. 1). In the laboratory, we correlated the cores VEG16-B, VEG16-1 and VEG16-2 using conspicuous lithostratigraphic layers to obtain an 840-cm long composite sediment sequence.

To establish the chronology of the sediment record, we submitted 12 terrestrial plant macrofossil samples for radiocarbon dating using accelerator mass spectrometry (AMS) to the Laboratory for the Analysis of Radiocarbon with AMS (LARA) of the University of Bern (Switzerland, Szidat et al., 2014). Radiocarbon dates were calibrated to calendar years using the IntCal20 calibration curve (Reimer et al., 2020). We then modelled the relationship between depth and age, fitting a smoothing spline (smoothing parameter: 0.25) to the accepted radiocarbon dates (sample BE-16304 at 540—536 cm depth was identified as an outlier and therefore excluded) using the 'clam' 2.3.9 package (Blaauw, 2010) running in R 4.0.5 (R Core Team, 2021). The section between 367 and 272 cm depth was considered as corresponding to a 'rapid deposition episode' based on the lithology (highly inorganic sediment consisting mainly of silt with bands of clay and turbidites), the radiocarbon dates constraining it and the very low pollen concentrations (Fig. 2), and thus excluded from the age-depth model (more details in the 'Results and Interpretation' section).

2.3 Palynological analysis

In the laboratory, we prepared 94 sediment samples of 1 cm^3 for palynological analysis using standard protocols (Moore et al., 1991), except mesh size for sieving was 500 μm. At the beginning of the treatment, we added a known quantity of *Lycopodium* spores to estimate pollen concentrations (Stockmarr, 1971). Later, pollen influx (= accumulation rate) was calculated dividing pollen concentration by the deposition time (yr cm^{-1}) derived from the age-depth model. We identified pollen grains and fern spores using dichotomous keys (Moore et al., 1991; Beug, 2004; Punt et al., 1976—2009), photographic atlases (Reille, 1992), and the reference collection at the *Institute of Plant Sciences* of the University of Bern (Switzerland) up to a minimum terrestrial pollen sum of 400 (mean $\pm$ SE = 484 $\pm$ 79). Additionally, we identified conifer stomata, fungal spores (including those of obligate coprophilous fungi) and other non-pollen palynomorphs (e.g. algae) using specific literature (e.g. Trautmann, 1953; van Geel et al., 2003; van Geel and Aptroot, 2006). Finally, we

quantified microscopic charcoal particles >10 μm in the pollen slides following Tinner and Hu (2003) and Finsinger and Tinner (2005). Non-pollen palynomorph and microscopic charcoal concentration and influx values were calculated as for pollen. Spore influx of obligate coprophilous fungi (in the Limni Vegoritis record, we found *Sporormiella* t. (t. = type), *Podospora* t. and *Delitschia* t.; Supplementary Data) is usually considered a proxy for the density of ungulates around lakes and mires (Gill et al., 2013; Baker et al., 2013, 2016), conifer stomata is a proxy for the local presence of trees (Ammann et al., 2014), and microscopic charcoal is a proxy for local to regional fire occurrence (Tinner et al., 1998; Conedera et al., 2009; Adolf et al., 2018).

2.4 Numerical analyses: zonation and ordination

We delimited statistically significant local pollen assemblage zones (LPAZ) applying the optimal partitioning using a sums-of-squares criterion (Birks, 2012) and the broken-stick model (Bennett, 1996) using PSIMPOLL 4.27 (Bennett, 2009).

To investigate the occurrence of underlying ecological gradients in the pollen data as well as to assess quantitatively the impact of fire occurrence and pastoral farming on the vegetation, we conducted unconstrained and constrained ordination analyses (Legendre and Birks, 2012) using Canoco 5 (ter Braak and Šmilauer, 2012). The dataset consists of 89 palynological samples, because the five samples within the 'rapid deposition episode' section were excluded. Given the rather short length-of-gradient of Axis 1 (1.51 standard deviation units of turnover) of a detrended correspondence analysis (DCA), we decided to use ordination methods based on linear response models (Legendre and Birks, 2012). To detect underlying ecological gradients in the multivariate percentage pollen dataset, we applied Principal Component Analysis (PCA; Legendre and Birks, 2012) on the square-root transformed pollen percentages. Regarding constrained ordination, we carried out a redundancy analysis (RDA; Legendre and Birks, 2012) to look into the responses of vegetation (percentage pollen data) to fire occurrence (microscopic charcoal influx) and

pastoral farming (*Sporormiella* t. influx). Only *Sporormiella* t. was considered because the other coprophilous fungi merely showed scattered occurrences (Supplementary Data). The statistical significance of the relationship between the pollen types (response variables) and the environmental variables (microscopic charcoal and *Sporormiella* t. influx) was tested using Monte Carlo permutation tests (999 iterations, reduced model, unrestricted permutations; Šmilauer and Lepš, 2014). Finally, we used the variation partitioning procedure (conditional effects tested) described in Šmilauer and Lepš (2014) to quantify the amount of variation in the pollen dataset explained by each environmental variable (fire occurrence and pastoralism) separately and jointly.

3. Results and interpretation

3.1 Lithostratigraphy and chronology

The sedimentary sequence of Limni Vegoritis mainly consists of calcareous clayey gyttja from the bottom (840-cm depth) up to 37-cm depth, interrupted by a thick section (367—272-cm depth) of highly inorganic sediment (silt, clay and turbidites), a pair of thinner layers of clay (243—231-cm depth) and a turbidite (180.5—176-cm depth; Fig. 2, Table S1). The uppermost 37 cm of the sequence are mainly gyttja (Fig. 2, Table S1). The age-depth model dates the bottom of the investigated sequence at ~9000 cal. BP (Fig. 2). Sediment accumulation rates are mostly between ~0.05 and 0.1 cm yr^{-1} until ~400-cm depth (estimated age ~1900 cal. BP), close to the lower limit of the highly inorganic sediment section (Fig. 2). The highly inorganic sediment composition suggests that this section was deposited very quickly during a particularly severe erosive stage. The partial overlap of the 95% confidence intervals of calibrated ages corresponding to the two radiocarbon dates that constrain the highly inorganic section of the sequence (BE-17475 and BE-16305 in Table 1) lends further support to the previous explanation. In line with this, pollen concentration drops to its lowest values in the entire record during the highly inorganic section, where pollen assemblages are very similar among them (Figs2—4). In summary, the various lines of

evidence available suggest that a 'rapid deposition episode' (probably consisting of several events occurring in close temporal proximity) associated with enhanced erosion led to the accumulation of a massive layer of highly inorganic sediment between 367 and 272-cm depth. From ~400-cm depth upwards sediment accumulation rates increase notably, ranging from ~0.1 to ~0.35 cm yr^{-1} (Fig. 2) .

3.2 Vegetation and fire history

The Limni Vegoritis pollen record was exceptionally diverse, with a total of 245 pollen and spore types of vascular plants. Seven statistically significant LPAZ (VEG-1 to VEG-7) were delimited and will be used to describe changes in vegetation and fire occurrence over the past ~9000 years (Figs 3—5).

During VEG-1 (840—788 cm; ~8990—8260 cal. BP), tree pollen increases from ~55% to ~70-75%, with *Quercus frainetto* t. and *Pinus sylvestris* t. as the most abundant taxa (Figs 3, 5). *Tilia*, *Ulmus*, *Betula*, *Corylus*, *Pistacia* and *Abies* feature continuous curves. Shrub pollen percentages fluctuate notably following the trends of the *Juniperus* t. curve. *Juniperus* t. is ~15% at the onset of the record, later decreases to <5% and finally increases again from ~8550 cal. BP to reach ~10% at the end of the zone, when *Arceuthobium oxycedri* pollen is also recorded (Fig. 3). Herb pollen percentages are usually around 20-25%, with Poaceae, *Artemisia*, Rubiaceae, *Rumex acetosa* t. and *Sanguisorba minor* t. as the most relevant taxa (Figs 4, 5). *Pteridium aquilinum* and Cyperaceae are the only fern and wetland plants reaching remarkable spore and pollen abundances, respectively (Figs 4, 5). Microscopic charcoal influx is ~4100-6200 # cm^{-2} yr^{-1} with a maximum ~9200 # cm^{-2} yr^{-1} at ~8550 cal. BP (Fig. 5). Meanwhile, only a couple of isolated spores of *Sporormiella* t. are recorded (Fig. 5). At ~9000 cal. BP the vegetation consisted of open woodlands with deciduous *Quercus*, *Pinus* and *Juniperus*. Later, these woodlands became more closed and diverse,

incorporating *Abies* and several deciduous broadleaved trees and shrubs. Fire occurrence was not significant and there is no evidence of arable or pastoral farming.

The decline of tree pollen (down to ~50%), chiefly featuring *Quercus frainetto* t., marks the transition to VEG-2 (788—700 cm; ~8260—6870 cal. BP; Figs 3, 5). Deciduous *Quercus* is mostly replaced by *Juniperus* t., which continues its increase that started at the end of VEG-1. Finds of *Juniperus* stomata support its local presence. Among the herbs, the most remarkable changes are the increases in *Artemisia*, *Polygonum aviculare* t. and Cichorioideae, as well as the continuous curve of *Rumex acetosella* t. (Fig. 5). Tree pollen percentages begin to recover at ~7900 cal. BP (~65-75%) driven by *Pinus nigra/sylvestris* t. (= *Pinus* subgenus *Pinus*). *Pinus* stomata occur when pine pollen abundances peak (Fig. 5). Following the initial decline, *Quercus frainetto* t. remains quite stable for several millennia (Fig. 5). The *Juniperus* t. increase culminates at ~8000—7900 cal. BP, then *Juniperus* t. decreases moderately and later shows another peak at ~7100 cal. BP, synchronous with a decrease in *Pinus nigra/sylvestris* t.. Poaceae continue as the most abundant herbaceous pollen, although slightly less abundant than in VEG-1 (Fig. 5). The Cerealia t. curve is continuous between ~8300—7650 cal. BP, while *Plantago lanceolata* t. and *Urtica dioica* t. show scattered occurrences. Microscopic charcoal influx shows an overall decreasing trend roughly from ~4000 to ~1000 # cm^{-2} yr^{-1}, punctuated by three maxima at ~8200 (~7950 # cm^{-2} yr^{-1}), 7750 (~7200 # cm^{-2} yr^{-1}) and 7250 (~4550 # cm^{-2} yr^{-1}) cal. BP (Fig. 5). The *Sporormiella* t. curve is continuous between ~8100—7650 and 7250—6950 cal. BP (Fig. 5). Initially, open deciduous oak-dominated woodlands were replaced by parkland-like vegetation consisting of steppe-like grasslands with sparse stands of *Juniperus*. Afterwards, pinewoods spread into the juniper parklands. The almost continuous record of cereal-like pollen and *Sporormiella* t., alongside the more regular occurrences of several secondary cultural indicators (weeds) suggest arable and pastoral farming activities. Increasing variability in the charcoal record also points to higher regional fire occurrence.

A marked rise in tree pollen (from ~65% to ~85%) occurs at the onset of VEG-3 (700—420 cm; ~6870—2110 cal. BP), mainly driven by *Pinus nigra/sylvestris* t. (Fig. 5). Tree pollen percentages remain ~80-90% until ~4500 cal. BP, when a gentle decreasing trend starts. *Pinus nigra/sylvestris* t. is the most abundant taxon overall, although two major drops occur at ~5950 and ~4200 cal. BP (Figs 5, S1). The relatively continuous record of *Pinus* stomata supports pine presence near the lake (Fig. 5). After this zone, *Pinus* stomata become rare. Similarly, the rather regular finds of *Loranthus europaeus* pollen support the local occurrence of deciduous *Quercus* stands as also suggested by *Quercus frainetto* t. pollen abundances (Fig. 3). *Ostrya carpinifolia* t., which is also produced by *Carpinus orientalis*, increases and then stays quite stable (Fig. 5). The stomatal record of *Juniperus* is rather continuous (Fig. 5). Other trees with continuous records are *Carpinus betulus*, *Fraxinus ornus* and *Abies*. The frequent occurrence of *Taxus* pollen is remarkable (Fig. 3). Also, the continuous and increasing representation of *Fagus* is worth noting. Poaceae continue as the most abundant herbaceous pollen. However, more remarkable are the continuous curves of Cerealia t., Brassicaceae, *Secale cereale* and *Cannabis sativa* t. feature continuous curves since ~4300, 4100, 2300 and 2300 cal. BP, respectively, and *Polygonum aviculare* t. increases since ~4200 cal. BP (Figs 3, 4, S1). Microscopic charcoal influx starts at <2000 # cm^{-2} yr^{-1}, reaches a maximum (~17,700 # cm^{-2} yr^{-1}) at ~5950 cal. BP, later stays ~4000-6000 # cm^{-2} yr^{-1} except for three maxima peaking at ~5000 (~11,900 # cm^{-2} yr^{-1}), ~2950 (~9700 # cm^{-2} yr^{-1}) and ~2600 cal. BP (~15,900 # cm^{-2} yr^{-1}), and finally drops to <2000 # cm^{-2} yr^{-1} (Fig. 5). The *Sporormiella* t. curve is continuous since ~4200 cal. BP, with a maximum (~280 spores cm^{-2} yr^{-1}) at ~2150 cal. BP (Fig. 5). During this LPAZ, forests and woodlands dominated by *Pinus* and deciduous *Quercus* were widespread. Other trees or shrubs such as *Juniperus*, *Abies*, *Ostrya carpinifolia*, *Carpinus orientalis*, *Carpinus betulus*, *Fraxinus ornus* and *Taxus baccata* also formed the canopy or the understory. Pinewoods declined several times but recovered afterwards. An increase in both arable and pastoral farming occurred at ~4300—

4200 cal. BP, coinciding with the beginning of woodland/forest clearance. Fire occurrence was notably higher.

A major drop in tree pollen (from >75% to ~25-30%) driven by abrupt *Pinus nigra/sylvestris* t. and *Abies* declines begins at ~2300 cal. BP and continues during VEG-4 (420—268 cm; ~2110—1660 cal. BP; Figs 5, S1). *Ostrya carpinifolia* t. decreases at ~1950 cal. BP. *Juniperus* t. increases abruptly, particularly after the 'rapid deposition episode', and has an almost continuous stomatal record. The highly diverse pollen assemblages include a suite of cultural indicators: Cerealia t. and *Secale cereale* as well as *Urtica dioica* t., *Rumex acetosella* t., *Plantago lanceolata* t. and *Polygonum aviculare* t. increase, and fruit trees such as *Castanea sativa*, *Juglans regia* and *Olea europaea* show continuous curves (Fig. 5). Additionally, the heliophilous fern *Pteridium aquilinum* largely expands (Fig. 5). Microscopic charcoal influx is ~1200-4250 # cm^{-2} yr^{-1}, whereas *Sporormiella* t. influx is ~40-160 spores cm^{-2} yr^{-1} (Fig. 5). Under increasing land-use intensity, conifer forests were cleared and replaced with pasturelands, croplands, and juniper woodlands probably managed as parklands.

Tree pollen partly recovers (mostly ~60-70%) during VEG-5 (268—176 cm; ~1660—960 cal. BP), with *Pinus nigra/sylvestris* t., *Fagus* and, to a lesser extent, *Ostrya carpinifolia* t. and *Quercus frainetto* t. as the main taxa involved (Figs 5, S1). This occurs partly at the expense of *Juniperus* t., which decreases significantly. At ~1400 cal. BP, tree pollen decreases moderately, due to *Fagus* declining. *Artemisia* follows a gradual increasing trend (Fig. 5). Microscopic charcoal influx is usually ~4000-10,000 # cm^{-2} yr^{-1}, while *Sporormiella* t. influx continues at ~30-120 spores cm^{-2} yr^{-1} (Fig. 5). Pine and oak woodlands recovered, probably partly recolonising their former territory outcompeting *Juniperus*, whereas at higher elevations *Fagus* expanded. Farming intensity probably decreased slightly, but the abundance and diversity of cultural indicators and the evidence suggestive of fire occurrence indicate continued land use.

At the beginning of VEG-6 (176—92 cm; ~960—290 cal. BP) tree pollen drops (from ~65% to ~25%), driven by the sudden and abrupt decrease in *Quercus frainetto* t., the less dramatic decline of *Pinus nigra/sylvestris* t., and a minor decrease in *Fagus* (Figs 5, S1). Tree pollen percentages never recover to previous values thereafter. In contrast, *Juniperus* t. begins a steady and consistent increase. Many other herbaceous taxa like *Artemisia*, Cichorioideae, *Polygonum aviculare* t., *Rumex acetosa* t., *Rumex acetosella* t. and *Urtica dioica* t. increase significantly (Figs 4, 5). Among the main cultural indicators, *Cannabis sativa* t. shows a maximum at ~650 cal. BP, *Castanea sativa* and *Plantago lanceolata* t. increase, *Papaver rhoeas* t. features an almost continuous curve, and both Cerealia t. and *Secale cereale* remain quite stable. The high relative abundance of *Pteridium aquilinum* spores is remarkable (Fig. 5). Microscopic charcoal influx values are mostly ~2000-5000 # cm^{-2} yr^{-1} (Fig. 5). In marked contrast, *Sporormiella* t. influx is overall >100 spores cm^{-2} yr^{-1}, with maxima up to ~500 spores cm^{-2} yr^{-1} (Fig. 5). Pine and oak woodlands were mostly cleared at the expense of crops and pasturelands. More specifically, steppe-like grasslands that make this area botanically renowned today seem to have established during this period. *Juniperus* (trees and/or shrubs) started to colonise these open habitats later.

Low tree pollen percentages characterise VEG-7 (92—0 cm; ~290 cal. BP—2016 CE) until the moderate increase driven by *Pinus nigra/sylvestris* t. and *Quercus frainetto* t. during the past few decades (Fig. 5). Nevertheless, the most noticeable feature of this zone is the dominance of *Juniperus* t. pollen. The cultivated trees *Castanea sativa*, *Olea europaea* and *Platanus* increase. Microscopic charcoal influx is mainly ~3000-5000 # cm^{-2} yr^{-1}, but *Sporormiella* t. influx values are ~100-450 spores cm^{-2} yr^{-1} (Fig. 5). Intense agricultural and pastoral farming continued, maintaining the landscape open for the entire period. *Juniperus* continued colonising the steppe-like grasslands to establish parklands, and more recently oak and pine woodlands slightly recovered.

3.3 Ordination

The first and second axes of the PCA explain 41.5% and 12.6% of the variation in the pollen dataset, respectively (Fig. 6a). PCA Axis 1 shows a gradient in vegetation openness associated with land use, with negative loads for taxa typical of woodlands and forests like *Pinus nigra/sylvestris* t., *Abies*, *Quercus frainetto* t. or *Taxus*, and positive loads for cultural indicators as well as *Juniperus* t. and Poaceae. PCA Axis 2 seems to be mainly driven by light availability (Ellenberg-type light indicator as compiled by Tichý et al., 2023), given that shade-tolerant taxa (*Fagus*, *Ostrya carpìnifolia* t. and *Carpinus betulus*) feature the most negative loads whereas light-demanding taxa (*Juniperus* t., *Corylus*, *Tilia* and *Ulmus*) show the most positive loads. Sample distribution in the PCA biplot shows a marked split between the LPAZ without noticeable anthropogenic influence (VEG-1 to VEG-3), where woodlands were usually dominant, and those reflecting heavier human impact (VEG-4, VEG-6 and VEG-7), where cultural indicators are more abundant and diverse. VEG-5 is located in-between, which highlights the incomplete recovery of woodland during this LPAZ and the major expansion of *Fagus* only recorded during this stage.

The results of the RDA show that microscopic charcoal and *Sporormiella* t. influx explain together 21.9% of the variation in the pollen dataset (F = 13.3, P = 0.001; Fig. 6b). Variation partitioning analysis shows that *Sporormiella* t. influx explains as much as 17.6% (F = 20.6, P = 0.001), charcoal influx only 1.4% (F = 2.6, P = 0.015), and the shared variance is 2.9%. Cultural indicators (e.g. Cerealia t., *Secale cereale*, *Plantago lanceolata* t.), disturbance-tolerant herbs (e.g. Cichorioideae, *Polygonum aviculare* t., *Artemisia*, *Urtica dioica* t.), and unpalatable browsing-resistant shrubs (*Juniperus* t.) are positively correlated with *Sporormiella* t. influx. Most forest trees like *Pinus nigra/sylvestris* t., *Abies*, *Quercus frainetto* t. or *Tilia*, which are sensitive to browsing/trampling, show negative correlations with *Sporormiella* t. influx. The relationship between microscopic charcoal influx and the different pollen types is less clear, probably because neat temporal trends in fire occurrence are lacking (Fig. 5). The proper interpretation and later discussion of the results of the RDA and the variation partitioning requires a comprehensive understanding of the relevant source

areas of the proxies used. On the one hand, the pollen and microscopic charcoal deposited in a mid-to-large-sized basin (*sensu* Sugita, 1994), like the subbasin of Limni Vegoritis studied here, mostly reflect distance-weighted vegetation composition and fire occurrence in the catchment and the broader region (10^3—10^4-m radius; Sugita, 1994; Tinner et al., 1998; Jackson and Lyford, 1999; Adolf et al., 2018). On the other hand, dung fungal spores such as *Sporormiella* t. usually come from shorter distances (10^1—10^3-m radius; Etienne et al., 2013; Gill et al., 2013; Baker et al., 2016), but inlet streams may amplify the source area. RDA results must therefore be taken with certain caution because of the imperfect match between the relevant source areas of the three proxies. Nevertheless, it also holds true that the abovementioned relevant source areas largely overlap and, additionally, we can assume that similar pastoral activities were widespread in the lake catchment.

4. Discussion

4.1 Climate-driven vegetation dynamics preceding farming

Mixed deciduous oak woodlands with *Pinus*, *Abies*, *Corylus*, *Tilia*, *Ulmus* and *Pistacia* among others, were the dominant vegetation around Limni Vegoritis ~9000 years ago. Regional proxy-based palaeoclimatic reconstructions show rather warm and subhumid conditions prevailing at that time (Fig. 5; Geraga et al., 2010; Göktürk et al., 2011; Francke et al., 2013; Tóth et al., 2015; Peckover et al., 2019). The remarkably close resemblance between the Limni Zazari (Gassner et al., 2020) and Limni Vegoritis pollen records during this period shows that the initial section of Limni Vegoritis marks the culmination of the delayed postglacial afforestation typical of northeastern Greece (Lawson et al., 2005; Kotthoff et al., 2008; Kouli et al., 2012; Masi et al., 2018; Gassner et al., 2020).

Deciduous *Quercus* started decreasing soon after reaching its maximum development (Figs 5, S1). During a first stage (~8600—8250 cal. BP), deciduous *Quercus* slightly declined, while *Abies*, *Juniperus* and *Corylus* expanded at its expense. During the second stage

(~8250—7900 cal. BP), steppe-like grasslands with abundant *Juniperus* trees/shrubs spread rapidly following the large sudden opening of mixed *Quercus* woodlands. This major vegetation shift occurred during the most significant Holocene 'rapid climate change' (RCC) event in the Adriatic and Aegean regions (~8600—8000(7800) cal. BP), which includes the '8.2 ka event' (Alley et al., 1997) and features a drop in sea surface temperatures (Rohling et al., 2019). The most abrupt decline of oak woodlands coincided with the coldest conditions recorded in marine sediments (Rohling and Pälike, 2005; Gogou et al., 2007; Marino et al., 2009; Triantaphyllou et al., 2016). In the southern Balkans and the eastern Mediterranean, the major cooling around the '8.2 ka event' was associated with the more frequent arrival and longer persistence of cold and dry air masses from central Eurasia, pushed southwards by the enhanced Siberian High (Rohling et al., 2002). Climate was particularly cold and dry in winter and early spring (Rohling and Pälike, 2005; Peckover et al., 2019). In marked contrast, regional chironomid-based summer temperature reconstructions show minor (Samartin et al., 2017) or no cooling (Tóth et al., 2015) during this period, but their time resolution is probably not sufficient to unambiguously identify short-lived cold spells like the '8.2 ka event'. Concerning water availability, the multi-proxy record of Lake Dojran suggests lower lake levels, colder temperatures and enhanced erosion between ~8300 and 7900 cal. BP (Francke et al., 2013). The $\delta^{13}C$ record of Sofular Cave speleothems also shows reduced precipitation and stronger seasonality in northern Anatolia between ~8400 and 7800 cal. BP, although here the reduction in precipitation was gradual (Fig. 5; Göktürk et al., 2011).

Enhanced dryness likely drove the replacement of mixed deciduous oak woodlands with wooded steppe, particularly if we assume that, like nowadays, the quite drought-sensitive *Quercus frainetto* was the dominant deciduous oak (Fyllas and Troumbis, 2009; Ripullone et al., 2020). Additionally, harsh winters and particularly late (spring) frosts may have severely damaged deciduous broadleaved trees and shrubs, even if the late phenology of submediterranean deciduous oaks (mainly *Quercus frainetto* and *Q. pubescens* in this area) makes them less prone to suffer significant damage (Pasta et al., 2016; Rubio-Cuadrado et

al., 2021). *Pinus* and *Juniperus* species currently growing in the area (*Pinus nigra*, *P. sylvestris*, *Juniperus communis*, *J. oxycedrus*, *J. excelsa*, *J. foetidissima*) are more frost-resistant, which would explain why they did not decline during this climatic reversal (Figs 5, S1; Fyllas and Troumbis, 2009; Bachofen et al., 2016). The impact of the RCC event centred by the '8.2 ka event' on the vegetation was variable across the southern Balkans (Denèfle et al., 2000; Lawson et al., 2004, 2005; Pross et al., 2009; Panagiotopoulos et al., 2013; Masi et al., 2018; Gassner et al., 2020; Brechbühl et al., 2024), probably depending on site elevation and continentality. Archaeological evidence suggests that the Neolithic began at ~8500 cal. BP in Greek Macedonia (Chrysostomou et al., 2015; Maniatis et al., 2015; Karamitrou-Mentessidi et al., 2015; Maniatis and Adaktylou, 2021). At Limni Vegoritis, the first scattered cereal-like pollen grains are recorded slightly later, alongside limited occurrences of the cultural indicators *Plantago lanceolata* t., *Urtica dioica* t. (Deza-Araujo et al., 2020), and the coprophilous fungus *Sporormiella*. This palynological evidence suggests small-scale and scattered Neolithic farming in the catchment ('garden-like' agriculture; Bogaard, 2005; Kouli, 2015), but does not explain the strong pollen-inferred woodland decline. However, further work aimed at increasing the time resolution of the record and especially at refining the taxonomic adscription of Cerealia t. pollen (Deza-Araujo et al., 2022) is necessary to get a more robust and comprehensive picture of early farming in the area.

4.2 The Holocene pinewoods of Northern Greece

The later woodland recovery, starting at ~7900 cal. BP, mostly involved the spread of pines into the steppe-like grasslands with junipers, likely in response to increased moisture availability and temperature (Fig. 5; Marino et al., 2009; Göktürk et al., 2011; Francke et al., 2013; Zhang et al., 2016). *Pinus* (co-)dominated forests persisted for several millennia (until ~2100 cal. BP) around Limni Vegoritis. Interestingly, the beginning of Bottema's (1982) Limni Vegoritis record is placed during this vegetation stage (Figure S2). Multi-millennial

Middle and Late Holocene pinewood dominance has also been recorded in other sites of the region (Denèfle et al., 2000; Lawson et al., 2005; Wagner et al., 2009; Kouli and Dermitzakis, 2010; Gassner et al., 2020) as well as in other continental areas of the Mediterranean region (Peñalba, 1994; Eastwood et al., 1999; Carrión, 2002; Morales-Molino et al., 2017). Most previous studies have discussed the moderately high abundances of *Pinus* pollen recorded during most of the Middle and Late Holocene in Northern Greece as associated with high-elevation pine forests (Lawson et al., 2005; Panagiotopoulos et al., 2013), because today pines only play a relevant role there (Bohn et al., 2000/2003; Senn et al., 2022). Nevertheless, the identity and spatial distribution of *Pinus* species in the regional woodlands and forests require further discussion in the light of the regular occurrence of *Pinus* stomata in the Limni Vegoritis palaeoecological record.

Pinus subgenus *Pinus*, to which belongs the vast majority of *Pinus* pollen in the Limni Vegoritis pollen record (*Pinus nigra/sylvestris* t. in Figs 3—6, S1), nowadays includes three species in the study area: *Pinus sylvestris*, *P. nigra* and *P. heldreichii*. In contrast, *Pinus* subgenus *Strobus* pollen is extremely rare (Supplementary Data). Today, *Pinus sylvestris*-dominated stands are widespread in the upper montane and subalpine vegetation belts and define the local timberline. Further, the treeline ecotone consists of subalpine scrub of *Juniperus communis* var. *saxatilis*, *Vaccinium myrtillus*, *Daphne oleoides* and *Erica spiculifolia* with scattered *P. sylvestris* trees (Quézel and Médail, 2003; Senn et al., 2022). *Pinus nigra* woods cover extensive areas at lower elevation (usually in submediterranean settings) on calcareous soils, for instance in the Olympus and Pindus Mountains (Quézel and Médail, 2003; Senn et al., 2022). Lastly, *Pinus peuce*, the only representative of *Pinus* subgenus *Strobus*, and *Pinus heldreichii* play an important role in the uppermost forests of the Balkan mountains, with their distribution constrained to small areas of the upper montane and subalpine belts (Quézel and Médail, 2003). *Pinus peuce* seems to have been quite rare throughout the Holocene. Similarly, the pollen representation of *Pinus heldreichii* in the Limni Vegoritis pollen assemblages must be limited considering that its very specific ecological

requirements result in a reduced potential niche. In contrast, high-elevation *Pinus sylvestris* woods must certainly have left their imprint in the Holocene pollen record. However, the high abundances of *Pinus* pollen recorded during the Middle and part of the Late Holocene do not match the reduced representation of today's well-developed and widespread high-elevation *Pinus sylvestris* stands in the Limni Vegoritis surface pollen sample (Fig. 5; Senn et al., 2022). Additionally, pollen records from high-elevation sites in the Voras Mountains strongly suggest that *Pinus sylvestris* did not experience there a sharp decline during the Late Holocene like the one that occurred at Limni Vegoritis (Fig. 5; Botema, 1982; Lawson et al., 2005; Gerasimidis et al., 2009). Furthermore, the rather continuous record of *Pinus* stomata in the small subbasin of Limni Vegoritis studied here (Figs 1, 5), which lacks any major inlet stream, is unlikely related to pinewoods located far away but rather to stands in the proximity to the lake (Ammann et al., 2014). Therefore, we consider *Pinus nigra* to have been the main pine species around Limni Vegoritis during the Holocene, thriving on the limestone hills that surround the lake. Marinova and Ntinou (2018) also considered this the most plausible explanation for the record of *Pinus sylvestris/P. nigra* charcoal in the Neolithic settlements of the region.

4.3 Pine and oak woodlands under increasing land use

Pinus nigra and deciduous *Quercus* (mainly *Quercus frainetto* and *Q. pubescens*, with less importance of *Q. cerris* and *Q. trojana*) dominated the forests and woodlands around Limni Vegoritis for more than 5000 years. Based on the pollen data, the ecology of the species and the local geomorphology, we suggest that: (i) pine-dominated stands thrived on steep slopes with shallower soils featuring lower water-holding capacity, (ii) oaks dominated on valley bottoms with deeper soils, and (iii) mixed stands with varying pine and oak abundances occurred in ecologically intermediate situations. Despite their relevance throughout this period, *Pinus nigra* woodlands also underwent several reductions. The first pine decline occurred at ~7100 cal. BP and involved a remarkable replacement of *Pinus nigra* with

Juniperus, probably on the driest sites. The second *Pinus nigra* decline occurred at ~5950 cal. BP and consisted of enhanced fire occurrence triggering the partial replacement of pines with deciduous oaks and grasslands. Our data do not support a human origin for such fire episodes, because both cultural indicator pollen and coprophilous fungi are almost lacking. In contrast, proxy data for moisture suggest that fire occurrence began to increase at the end of a dry period that lasted for a few centuries (Fig. 5; Göktürk et al., 2011). A third decrease in *Pinus* abundances is dated to ~4200 cal. BP and will be discussed in detail below.

During this long forest stage (~6900—2300 cal. BP) the local woodlands hosted a notable diversity of trees, with *Abies* and *Juniperus* as the main conifers alongside *Pinus*. Among the hardwoods, several taxa that were relatively abundant during the Early Holocene (e.g. *Ulmus*, *Tilia*, *Fraxinus*) continued declining. Regionally, deciduous oak woodlands attained their maximum importance between ~6000 and 5400 cal. BP, benefitting from a period of low inferred human population density (Weiberg et al., 2019). In other submediterranean mountains of Southern Europe, these deciduous broadleaved trees also declined, mainly because of increasing anthropogenic disturbance (Tinner et al., 1999; Vescovi et al., 2010; Morales-Molino et al., 2021; Lang et al., 2023). At Limni Vegoritis evidence of human impact is scarce for this period (Fig. 5). However, although Neolithic settlers had a limited impact in the broad landscape, they could have heavily exploited certain floodplain areas particularly suitable for farming activities because of their high water table, where these mesophytes (*Ulmus*, *Tilia*, *Fraxinus*) were growing (Marinova and Ntinou, 2018). In contrast, *Ostrya carpinifolia/Carpinus orientalis* and *Carpinus betulus* notably expanded from ~7500 cal. BP onwards (Figs 5, S1), playing an important role in the *Pinus-Quercus* woodlands. The Mid-Holocene expansion of *Ostrya carpinifolia/Carpinus orientalis* was a widespread and remarkable process in the southern Balkans known for a long time (Willis, 1994). We suggest that anthropogenic disturbance (even if slight) played a role in assisting this spread (see Brechbühl et al., 2024), because the strong resprouting capacity of both *Ostrya carpinifolia* and *Carpinus orientalis* allow a rapid post-disturbance recovery (Gobet et al.,

2000). Lastly, the expansion of *Fagus* began later (at ~5200 cal. BP) following a maximum in fire occurrence (at ~5300 cal. BP), like in Limni Zazari (Gassner et al., 2020). Beech probably established in the upper *Pinus nigra* and deciduous *Quercus* (in moist sites such as ravines or shady slopes) and/or the lower *Pinus sylvestris* belts. The initial *Fagus* establishment occurred under cool and moist conditions (Fig. 5; Marino et al., 2009; Göktürk et al., 2011; Tóth et al., 2015). Interestingly, during the major development of *Fagus* stands, between ~1600 and 1000 cal. BP, climate was slightly drier (Fig. 5; Göktürk et al., 2011) and fire occurrence and pastoral farming were stronger than during their initial establishment ~5000 cal. BP (Fig. 5). Anthropogenic disturbance, involving heavier pastoralism and fire occurrence have also favoured beech spread at other European sites (Bradshaw and Lindbladh, 2005; Tinner and Lotter, 2006; Morales-Molino et al., 2021; Cagliero et al., 2022).

The abovementioned pine decline dated at ~4200 cal. BP deserves further scrutiny because the '4.2 ka event' reportedly had a significant impact on the Mediterranean realm (Bini et al., 2019). In the southern Balkans, the '4.2 ka event' featured drier (Francke et al., 2013; Finné et al., 2017; Psomiadis et al., 2018) and cooler conditions (Bini et al., 2019), although robust and widespread evidence supporting the latter is lacking (Ön, 2023). In line with this, the $\delta^{13}C$ curve from the Sofular Cave speleothems also shows a trend towards drier conditions between ~5000 and 4200 cal. BP (Fig. 5; Göktürk et al., 2011). Around Limni Vegoritis, deciduous *Quercus*, *Ostrya carpinifolia*, *Carpinus orientalis* and *Carpinus betulus* spread at the expense of *Pinus nigra* during this period, whereas *Fagus* stands slightly expanded at higher elevations (Figs 5, S1). Synchronous increases in the abundances of coprophilous fungi (chiefly *Sporormiella* t.) and several cultural indicators (e.g., Cerealia t., *Polygonum aviculare* t., *Plantago lanceolata* t.) indicate increased land use (pastoral and arable farming) intensity during the Bronze Age, which might have cause pinewood clearance (Fig. 5). All the abovementioned woody taxa that replaced pines resprout vigorously (San-Miguel-Ayanz et al., 2016), which would have allowed them not only to cope with the disturbance causing the pine decline but to benefit from it and spread in the woodlands. Regionally, most forest

clearance episodes occurring during this period were also related to increased land use (Masi et al., 2018; Weiberg et al., 2019; Gassner et al., 2020; Glais et al., 2023). Further, the first major forest clearance episode at Limni Zazari occurred during the Bronze Age and affected fundamentally *Pinus* (Gassner et al., 2020). In marked contrast, oak woodlands were way more affected by Bronze Age anthropogenic forest clearance elsewhere in Northern Greece, with pinewoods partly colonising their former range (Weiberg et al., 2019).

The recovery of *Pinus nigra* to pre-disturbance conditions, replacing deciduous *Quercus*, *Ostrya carpinifolia*, *Carpinus orientalis*, and *Carpinus betulus*, took ~1000 years from ~4200 to 3200 cal. BP under low land-use intensity. High *Pinus nigra/sylvestris* t. pollen percentages but especially the continuous record of stomata indicate that *Pinus nigra* played a fundamental role in the local to extra-local vegetation. *Pinus* and to a lesser extent *Abies* spread further at the transition between the Bronze Age and 'Ancient Greece' period (which embraces the Iron Age and the Archaic, Classical and Hellenistic periods, i.e. ~3100—2100 cal. BP; Roberts et al., 2011). The conifer forest expansion at ~3100 cal. BP at Limni Vegoritis constitutes one of the most striking differences with the Limni Zazari record, as the first major anthropogenic deforestation event occurred at the Limni Zazari at the onset of the Iron Age (= early 'Ancient Greece') and mostly involved a gradual decline of *Pinus* (Gassner et al., 2020). Like at Limni Zazari, other regional palaeoecological records show widespread forest clearance associated with intensified land use during the Bronze Age and especially at the Bronze Age-Ancient Greece transition (~3200—3100 cal. BP; Willis, 1992a, b; Denèfle et al., 2000; Glais et al., 2016, 2023; Cruz-Silva et al., 2024). The subsequent Classical Antiquity period is characterised at Limni Vegoritis by higher fire occurrence but lighter pastoralism, under prevailing dry and cool conditions (Fig. 5; Göktürk et al., 2011; Finné et al., 2014, 2017). RDA suggests that higher livestock densities seem to have negatively affected *Pinus* and *Abies* at our study site (Fig. 6b). Livestock reduction would therefore have enabled pine and fir recruitment. Although higher resolution charcoal data would be desirable to get more robust insights into the past regional fire regime, we suggest that

charcoal maxima during this period are associated with surface fires because: (i) *Pinus nigra*, which was hardly affected by wildfires, can withstand surface fires but crown fires are lethal (Tapias et al., 2004; Christopoulou et al., 2013; Ne'eman and Arianoutsou, 2021); (ii) *Abies*, which is very sensitive to fire (Mauri et al., 2016; Caudullo and Tinner, 2016), was unaffected and even spread slightly; and, (iii) deciduous *Quercus*, which were probably growing in the understory of pinewoods, significantly declined. Farming remained at low intensity for most of the 'Ancient Greece' cultural period to increase slightly between ~2900—2400 cal. BP (higher abundance of apophytes and cereals; Deza-Araujo et al., 2020).

4.4 The strong legacy of land use during the past two millennia on the modern landscape

Thus far, the Limni Vegoritis palaeoecological record has already shown several significant vegetational changes. However, it is over the past ~2500-2000 years when the most abrupt shifts have occurred (Figs 5, 6), which have in turn left strong imprints on the modern landscape of Northern Greece. The sharpest vegetation change started at ~2300 cal. BP and was realised ~2100 cal. BP, roughly coinciding with the late 'Ancient Greece' period and particularly Roman Times. On the one hand, *Pinus nigra* and *Abies* were almost extirpated from the study area. On the other hand, *Juniperus* parklands, fruit tree orchards (*Castanea sativa*, *Juglans regia*) and cereal fields (Cerealia t. and particularly *Secale cereale*) expanded. This dramatic vegetation shift occurred under increased pastoralism, which seems to have had a strong impact on pine and fir, but it could also have involved logging. Comparing the abundance of *Pinus nigra/sylvestris* t. in the post-deforestation event pollen assemblages with the modern pollen-vegetation regional dataset (Senn et al., 2022), even high-elevation pine forests dominated by *Pinus sylvestris* might have been affected by land-use intensification. However, relatively close high-elevation sites record *Abies* declines, but only slight reductions of *Pinus* at that time (Lawson et al., 2005; Gerasimidis et al., 2009). The magnitude of the above-described vegetation change is clearly reflected in the PCA

biplot (transition between VEG-3 and VEG-4; Fig. 6a). Further, the close proximity between the VEG-4 (Roman Times) and VEG-7 (past 300 years) pollen assemblages in the PCA clearly illustrates the magnitude of Roman land-use impact on the vegetation (Fig. 6a). Bottema's (1982) pollen sequence shows the same patterns of vegetation change (Figure S2). Heavy deforestation largely enhanced erosion in the catchment, which resulted in the 'rapid deposition episode', i.e. the quick deposition of a massive layer of mainly inorganic sediment (Fig. 2). Available palaeoecological evidence shows that anthropogenic ecosystem disturbance was heaviest in the southern Balkans during the past ~2500—2000 years (Lawson et al., 2005; Panagiotopoulos et al., 2013; Zhang et al., 2016; Masi et al., 2018). Similarly, strong human-induced *Pinus* and *Abies* forest declines occurred during the same period in other mountainous regions of Southern Europe (e.g. Franco Múgica et al., 2001; Vescovi et al., 2010; Morales-Molino et al., 2017, 2021, 2022).

Following the 'rapid deposition episode', woodlands partially recovered during the early Byzantine period, but with a substantially different composition (Fig. 6a). The moderate re-expansion of *Pinus* coupled with the notable spread of *Fagus* suggest that mixed *Pinus*-*Fagus* forests established in the former domain of montane pinewoods. At Rezina marsh *Pinus* woods were also quite resilient to anthropogenic disturbance (Willis, 1992b). At lower elevations, deciduous *Quercus* continued playing a major role in the woods, probably mixed with pines. *Juniperus* underwent a striking decline that can be explained by oaks and pines benefitting from the slight decrease in land-use intensity to spread and subsequently outcompete junipers. This explanation matches the unchanged abundances of Poaceae and other taxa typical of steppe-like grasslands (mainly *Artemisia*). The curve of *Platanus* is continuous only from ~1400 cal. BP, which points to an anthropogenic origin in this area.

Finally, at ~1000 cal. BP the remnants of lowland deciduous *Quercus*-*Pinus* woodlands were definitively cleared (Figs 5, S1). *Pinus* declined more gradually than deciduous *Quercus*, probably because most pinewoods were growing at high-elevation and were therefore less affected by increased land use. Considering the chronological uncertainty of

the uppermost section of the core, the final rise in *Pinus* pollen abundance alongside the finding of some *Pinus* stomata may well correspond to recent pine afforestation during the past few decades (Fig. 5). *Fagus* stands that were also at higher elevation remained undisturbed. According to *Sporormiella* t. influx, pastoral farming started increasing, which agrees with the increasing abundances of apophytes (e.g. *Plantago lanceolata* t., *Polygonum aviculare* t., *Urtica dioica* t.). Similarly, *Castanea sativa* cultivation also developed in the region during this period on acidic soils, like in other submediterranean areas of Southern Europe (Conedera et al., 2004; Morales-Molino et al., 2015). Lastly, the current cultural landscape of the hills around Limni Vegoritis, characterised by heavily grazed steppe-like grasslands with scattered *Juniperus* trees/shrubs, cereal fields, degraded oak woodlands, and *'shibljak'* has developed over the past few centuries. Similar vegetation dynamics occurred around Limni Zazari (Gassner et al., 2020) and Nisi Fen (Lawson et al., 2005), but without the massive spread of *Juniperus* observed at Limni Vegoritis.

5. Conclusions

The new paleoecological record of Limni Vegoritis clearly illustrates the interplay between climatic and anthropogenic drivers in defining the landscape of Northern Greece at centennial to millennial timescales. First, the notably cooler and drier conditions that characterised the RCC event centred around the '8.2 ka event' in this inland area of Northern Greece would explain the major forest opening in the study area. Palynological evidence points to small-scale Neolithic farming in the lake catchment, in agreement with regional archaeobotanical evidence of 'garden-like' agriculture (Bogaard, 2005; Kouli, 2015). In any case, to better address this question, future palaeoecological research in the area will require higher temporal and taxonomic resolution to disclose further interesting insights into the impact of early farmers on the vegetation of Northern Greece. At the end of the RCC event, pines spread in the area to (co-)dominate the woodlands. We conclude that these pinewoods developed at mid-elevation slopes and the pine species involved was *Pinus*

nigra. These pine-dominated woodlands persisted for several millennia under low to moderate land-use intensity, but land-use intensification during late 'Ancient Greece' and especially Roman Times, involving mainly pastoralism but probably also woodland exploitation for timber production, caused the rapid collapse of conifer forests (*Pinus*, *Abies*). This process meant the demise of a 'foundation tree species' (Ellison et al., 2005) over extensive areas, which led to a shift to another stable state in which hardwood species became dominant. Renewed and strengthened land use during the past millennium caused further woodland clearance and the current configuration of the landscape, with cereal fields, heavily grazed steppe-like grasslands with junipers and open degraded oak woodlands. Our data reveal that land use has been the main driver of vegetation change in Northern Greece for at least the past two millennia. The palaeoecological evidence presented agrees with previous studies (Bottema, 1982; Gassner et al., 2020), but is in marked disagreement with Cruz-Silva et al. (2024), who stated that moisture availability has been the dominant ecological factor controlling vegetation dynamics in this region over long timescales. Our results also clearly depict the strong legacy of past land use on the extant vegetation of submediterranean Greece, as even vegetation types that were dominant until quite recently such as mid-elevation pinewoods vanished. The consequences of the long-lasting legacy of land-use history are relevant for future ecosystem adaptation to climate change (Vilà-Cabrera et al., 2023).

CRediT author statement

C.M.-M.: Conceptualization, Formal analysis, Investigation, Data curation, Visualization, Writing – Original draft. **L.v.V:** Visualization, Writing – Review and editing. **J.F.N.v.L., E.G., A.F.L.:** Investigation, Writing – Review and editing. **C.S., K.G., T.G., S.O.B.:** Writing – Review and editing. **A.B., A.H., K.K.:** Project administration, Funding acquisition, Writing – Review and editing. **W.T.:** Conceptualization, Project administration, Funding acquisition, Writing – Review and editing.

Declaration of competing interests

The authors declare that they have no known competing financial interests or personal relationships that could have appeared to influence the work reported in this paper.

Data availability

The datasets are archived in the Alpine Pollen Database and are freely accessible via the Neotoma Paleoecology Database (www.neotomadb.org).

Funding

This research has been conducted within the ERC Synergy project 'EXPLO: Exploring the dynamics and causes of prehistoric land use change in the cradle of European farming' (Grant Agreement No. 810586) funded by the European Research Council. The initial fieldwork campaign was funded by the University of Bern (ID-Grant 2015/003). Additionally, C.M.-M. was supported by an 'Atracción de Talento Modalidad 1' grant (2022-T1/AMB-23788) funded by the Comunidad de Madrid region.

Acknowledgements

We would like to express our sincere gratitude to Willi Tanner and Sebastian Eggenberger for their help with coring. We thank the Hellenic Survey of Geology and Mineral Exploration (HSGME) for the coring permit.

References

Adolf, C., Wunderle, S., Colombaroli, D., Weber, H., Gobet, E., Heiri, O., et al., 2018. The sedimentary and remote-sensing reflection of biomass burning in Europe. Global Ecology and Biogeography 27, 199-212.

Alley, R.B., Mayewski, P.A., Sowers, T., Stuiver, M., Taylor, K.C., Clark, P.U., 1997. Holocene climatic instability: A prominent, widespread event 8200 yr ago. Geology 25, 483-486.

Ammann, B., van der Knaap, W.O., Lang, G., Gaillard, M.-J., Kaltenrieder, P., Rösch, M., et al., 2014. The potential of stomata analysis in conifers to estimate presence of conifer trees: examples from the Alps. Vegetation History and Archaeobotany 23, 249-264.

Bachofen, C., Wohlgemuth, T., Ghazoul, J., Moser, B., 2016. Cold temperature extremes during spring do not limit the range shift of Mediterranean pines into regions with intermittent frost. Functional Ecology 30, 856-865.

Baker, A.G., Bhagwat, S.A., Willis, K.J., 2013. Do fungal spores make a good proxy for past distribution of large herbivores? Quaternary Science Reviews 62, 21-31.

Baker, A.G., Cornelissen, P., Bhagwat, S.A., Vera, F.W.M., Willis, K.J., 2016. Quantification of population sizes of large herbivores and their long-term functional role in ecosystems using dung fungal spores. Methods in Ecology and Evolution 7, 1273-1281.

Bennett, K.D., 1996. Determination of the number of zones in a biostratigraphical sequence. New Phytologist 132, 155-170.

Bennett, K.D., 2009. Documentation for Psimpoll 4.27 and Pscomb 1.03. C Programs for Plotting and Analyzing Pollen Data. The 14Chrono Centre, Archaeology and Palaeoecology, Queen's University of Belfast, Belfast, UK.

Betti, L., Beyer, R.M., Jones, E.R., Eriksson, A., Tassi, F., Siska, V., et al., 2020. Climate shaped how Neolithic farmers and European hunter-gatherers interacted after a major slowdown from 6,100 BCE to 4,500 BCE. Nature Human Behaviour 4, 1004-1010.

Beug, H.-J., 2004. Leitfaden der Pollenbestimmung fur Mitteleuropa und angrezende Gebiete. F. Pfeil Verlag, Munchen, Germany.

Bini, M., Zanchetta, G., Persoiu, A., Cartier, R., Català, A., Cacho, I., et al., 2019. The 4.2 ka BP Event in the Mediterranean region: an overview. Climate of the Past 15, 555-577.

Birks, H.J.B., 2012. Analysis of stratigraphical data. In: Birks, H.J.B., Lotter, A.F., Juggins, S., Smol, J.P. (eds.), Tracking environmental change using lake sediments volume 5: Data handling and numerical techniques, Springer, Dordrecht, The Netherlands, pp. 355-378.

Blaauw, M., 2010. Methods and code for 'classical' age-modelling of radiocarbon sequences. Quaternary Geochronology 5, 512-518.

Bogaard, A., 2005. 'Garden agriculture' and the nature of early farming in Europe and the Near East. World Archaeology 37, 177-196.

Bohn, U., Neuhausl, R., Gollub, G., Hettwer, C., Neuhauslova, Z., Raus, T., et al., 2000/2003. Map of the natural vegetation of Europe. Scale 1:2,500,000. Federal Agency for Nature Conservation, Munster, Germany.

Bottema, S., 1974. Late Quaternary Vegetation History of Northwestern Greece. PhD thesis, Groningen, 190 pp.

Bottema, S., 1982. Palynological investigations in Greece with special reference to pollen as an indicator of human activity. Palaeohistoria 24, 257-289.

Bradshaw, R.H.W., Lindbladh, M., 2005. Regional spread and stand-scale establishment of *Fagus sylvatica* and *Picea abies* in Scandinavia. Ecology 86, 1679-1686.

Brechbühl, S., van Vugt, L., Gobet, E., Morales-Molino, C., Volery, J., Lotter, A.F., et al., 2024. Vegetation dynamics and land-use change at the Neolithic lakeshore settlement site of Ploča Mičov Grad, Lake Ohrid, Macedonia. Vegetation History and Archaeobotany 33, 247-267.

Cagliero, E., Morresi, D., Paradis, L., Curovic, M., Spalevic, V., Marchi, N., et al., 2022. Legacies of past human activities on one of the largest old-growth forests in the south-east European mountains. Vegetation History and Archaeobotany 31, 415-430.

Carrión, J.S., 2002. Patterns and processes of Late Quaternary environmental change in a montane region of southwestern Europe. Quaternary Science Reviews 21, 2047-2066.

Caudullo, G., Tinner, W., 2016. *Abies* – Circum-Mediterranean firs in Europe: distribution, habitat, usage and threats. In: San-Miguel-Ayanz, J., de Rigo, D., Caudullo, G., Houston Durrant, T., Mauri, A. (eds.), European atlas of forest tree species, Publication Office of the European Union, Luxembourg, pp. 50-51.

Christopoulou, A., Fulé, P.Z., Andriopoulos, P., Sarris, D., Arianoutsou, M., 2013. Dendrochronology-based fire history of *Pinus nigra* forests in Mount Taygetos, Southern Greece. Forest Ecology and Management 293, 132-139.

Chrysostomou, P., Jagoulis, T., Mader, A., 2015. The 'Culture of Four Lakes': prehistoric lakeside settlements (6th-2nd millennium BC) in the Amindeon Basin, Western Macedonia, Greece. Archaologie Schweiz 38, 24-32.

Conedera, M., Krebs, P., Tinner, W., Pradella, M., Torriani, D., 2004. The cultivation of *Castanea sativa* Mill. in Europe, from its origin to its diffusion on a continental scale. Vegetation History and Archaeobotany 13, 161-179.

Conedera, M., Tinner, W., Neff, C., Meurer, M., Dickens, A.F., Krebs, P., 2009. Reconstructing past fire regimes: methods, applications, and relevance to management and conservation. Quaternary Science Reviews 28, 435-456.

Cruz-Silva, E., Harrison, S.P., Prentice, I.C., Marinova, E., 2024. Holocene vegetation dynamics of the Eastern Mediterranean region: Old controversies addressed by a new analysis. Journal of Biogeography 51, 294-310.

Denèfle, M., Lézine, A.M., Fouache, E., Dufaure, J.-J., 2000. A 12,000-year pollen record from Lake Maliq, Albania. Quaternary Research 54, 423-432.

Deza-Araujo, M., Morales-Molino, C., Tinner, W., Henne, P.D., Heitz, C., Pezzatti, G.B., et al., 2020. A critical assessment of human-impact indices based on anthropogenic pollen indicators. Quaternary Science Reviews 236, 106291.

Deza-Araujo, M., Morales-Molino, C., Conedera, M., Pezzatti, G.B., Pasta, S., Tinner, W., 2022. Influence of taxonomic resolution on the value of anthropogenic pollen indicators. Vegetation History and Archaeobotany 31, 67-84.

Donders, T., Panagiotopoulos, K., Koutsodendris, A., Bertini, A., Mercuri, A.M., Masi, A., et al., 2021. 1.36 million years of Mediterranean forest refugium dynamics in response to glacial-interglacial cycle strength. Proceedings of the National Academy of Sciences of the United States of America 118, e2026111118.

Doulgeris, C., Argyroudi, A., 2019. Contribution to decision-making on establishing the maximum water level for Lake Vegoritida. Lakes and Reservoirs 24, 24-36.

Eastwood, W.J., Roberts, N., Lamb, H.F., Tibby, J.C., 1999. Holocene environmental change in southwest Turkey: a palaeoecological record of lake and catchment-related changes. Quaternary Science Reviews 18, 671-695.

Ellison, A.M., Bank, M.S., Clinton, B.D., Colburn, E.A., Elliott, K., Ford, C.R., et al., 2005. Loss of foundation species: consequences for the structure and dynamics of forested ecosystems. Frontiers in Ecology and the Environment 3, 479-486.

Etienne, D., Wilhelm, B., Sabatier, P., Reyss, J.-L., Arnaud, F., 2013. Influence of sample location and livestock numbers on *Sporormiella* concentrations and accumulation rates in surface sediments of Lake Allos, French Alps. Journal of Paleolimnology 49, 117-127.

Feurdean, A.N., Willis, K.J., Astalos, C., 2009. Legacy of the past land-use changes and management on the 'natural' upland forest composition in the Apuseni Natural Park, Romania. The Holocene 19, 967-981.

Feurdean, A., Tonkov, S., Pfeiffer, M., Panait, A., Warren, D., Vannière, B., Marinova, E., 2019. Fire frequency and intensity associated with functional traits of dominant forest type in the Balkans during the Holocene. European Journal of Forest Research 138, 1049-1066.

Finné, M., Bar-Matthews, M., Holmgren, K., Sundqvist, H.S., Liakopoulos, I., Zhang, Q., 2014. Speleothem evidence for late Holocene climate variability and floods in Southern Greece. Quaternary Research 81, 213-227.

Finné, M., Holmgren, K., Shen, C.-C., Hu, H.-M., Boyd, M., Stocker, S., 2017. Late Bronze Age climate change and the destruction of the Mycenaean Palace of Nestor at Pylos. PLoS ONE 12, e0189447.

Finsinger, W., Tinner, W. 2005. Minimum count sums for charcoal-concentration estimates in pollen slides: Accuracy and potential errors. The Holocene 15, 293-297.

Fleitmann, D., Cheng, H., Badertscher, S., Edwards, R.L., Mudelsee, M., Göktürk, O.M., et al., 2009. Timing and climatic impact of Greenland interstadials recorded in stalagmites from northern Turkey. Geophysical Research Letters 36, L19707.

Fletcher, W.J., Müller, U.C., Koutsodendris, A., Christanis, K., Pross, J., 2013. A centennial-scale record of vegetation and climate variability from 312 to 240 ka (Marine Isotope Stages 9c—a, 8 and 7e) from Tenaghi Philippon, NE Greece. Quaternary Science Reviews 78, 108-125.

Foster, D., Swanson, F., Aber, J., Burke, I., Brokaw, N., Tilman, D., Knapp, A., 2003. The importance of land-use legacies to ecology and conservation. BioScience 53, 77-88.

Francke, A., Wagner, B., Leng, M.J., Rethemeyer, J., 2013. A Late Glacial to Holocene record of environmental change from Lake Dojran (Macedonia, Greece). Climate of the Past 9, 481-498.

Franco Múgica, F., García Antón, M., Maldonado Ruiz, J., Morla Juaristi, C., Sainz Ollero, H., 2001. The Holocene history of *Pinus* forests in the Spanish Northern Meseta. The Holocene 11, 343-358.

Fyllas, N.M., Troumbis, A.Y., 2009. Simulating vegetation shifts in north-eastern Mediterranean mountain forests under climatic change scenarios. Global Ecology and Biogeography 18, 64-77.

Gassner, S., Gobet, E., Schwörer, C., van Leeuwen, J., Vogel, H., Giagkoulis, T., et al., 2020. 20,000 years of interactions between climate, vegetation and land use in Northern Greece. Vegetation History and Archaeobotany 29, 75-90.

Geraga, M., Ioakim, C., Lykousis, V., Tsaila-Monopolis, S., Mylona, G., 2010. The high-resolution palaeoclimatic and palaeoceanographic history of the last 24,000 years in the central Aegean Sea, Greece. Palaeogeography, Palaeoclimatology, Palaeoecology 287, 101-115.

Gerasimidis, A., Athanasiadis, N., Panajiotidis, S., 2009. Contributions to the European Pollen Database: 8. Mount Voras (north-west Greece). Grana 48, 316-318.

Gerasimidis, A., Panajiotidis, S., 2010. Contributions to the European Pollen Database: 9. Flambouro, Pieria Mountains (northern Greece). Grana 49, 76-78.

Gill, J.L., McLauchlan, K.K., Skibbe, A.M., Goring, S., Zirbel, C.R., Williams, J.W., 2013. Linking abundances of the dung fungus *Sporormiella* to the density of bison: implications for assessing grazing by megaherbivores in palaeorecords. Journal of Ecology 101, 1125-1136.

Glais, A., López-Sáez, J.A., Lespez, L., Davidson, R., 2016. Climate and human-environment relationships on the edge of the Tenaghi-Philippon marsh (Northern Greece) during the Neolithization process. Quaternary International 403, 237-250.

Glais, A., Lespez, L., Vannière, B., López-Sáez, J.A., 2017. Human-shaped landscape history in NE Greece. A palaeoenvironmental perspective. Journal of Archaeological Science: Reports 15, 405-422.

Glais, A., Lespez, L., López-Sáez, J.A., Tsirtsoni, Z., Virmoux, C., Ghilardi, M., et al., 2023. Rapid climate changes and human dynamics during the Holocene in the eastern

Mediterranean (Lower Strymon Valley, northern Greece). Quaternary Science Reviews 313, 108130.

Gobet, E., Tinner, W., Hubschmid, P., Jansen, I., Wehrli, M., Ammann, B., Wick, L., 2000. Influence of human impact and bedrock differences on the vegetational history of the Insubrian Southern Alps. Vegetation History and Archaeobotany 9, 175-187.

Gogou, A., Bouloubassi, I., Lykousis, V., Arnaboldi, M., Gaitani, P., Meyers, P.A., 2007. Organic geochemical evidence of Late Glacial—Holocene climate instability in the North Aegean Sea. Palaeogeography, Palaeoclimatology, Palaeoecology 256, 1-20.

Göktürk, O.M., Fleitmann, D., Badertscher, S., Cheng, H., Edwards, R.L., Leuenberger, M., et al., 2011. Climate on the southern Black Sea coast during the Holocene: implications from the Sofular Cave record. Quaternary Science Reviews 30, 2433-2445.

Hofmanová, Z., Kreutzer, S., Hellenthal, G., Sell, C., Diekmann, Y., Díez-del-Molino, D., et al., 2016. Early farmers from across Europe directly descended from Neolithic Aegeans. Proceedings of the National Academy of Sciences of the United States of America 113, 6886-6891.

Jackson, S.T., Lyford, M.E., 1999. Pollen dispersal models in Quaternary plant ecology: assumptions, parameters, and prescriptions. The Botanical Review 65, 39-75.

Karamitrou-Mentessidi, G., Efstratiou, N., Kaczanowska, M., Kozlowski, J., 2015. Early Neolithic settlement of Mavropigi in Western Greek Macedonia. Eurasian Prehistory 12, 47-116.

Kotthoff, U., Müller, U.C., Pross, J., Schmiedl, G., Lawson, I.T., van de Schootbrugge, B., Schulz, H., 2008. Lateglacial and Holocene vegetation dynamics in the Aegean region: an integrated view based on pollen data from marine and terrestrial archives. The Holocene 18, 1019-1032.

Kouli, K., Dermitzakis, M.D., 2010. Contributions to the European Pollen Database: 11. Lake Orestias (Kastoria, northern Greece). Grana 49, 154-156.

Kouli, K., Gogou, A., Bouloubassi, I., Triantaphyllou, M.V., Ioakim, C., Katsouras, G., Roussakis, G., Lykousis, V., 2012. Late postglacial paleoenvironmental change in the northeastern Mediterranean region: Combined palynological and molecular biomarker evidence. Quaternary International 261, 118-127.

Kouli, K., 2015. Plant landscape and land use at the Neolithic lake settlement of Dispilió (Macedonia, northern Greece). Plant Biosystems 149, 195-204.

Lang, G., Ammann, B., van der Knaap, W.O., Morales-Molino, C., Schwörer, C., Tinner, W., 2023. Regional vegetation history. In: Lang, G., Ammann, B., Behre, K.-E., Tinner, W. (eds.), Quaternary vegetation dynamics of Europe, Haupt, Bern, Switzerland, pp. 150-246.

Lawson, I.T., Frogley, M., Bryant, C., Preece, R., Tzedakis, P., 2004. The Lateglacial and Holocene environmental history of the Ioannina basin, north-west Greece. Quaternary Science Reviews 23, 1599-1625.

Lawson, I.T., Al-Omari, S., Tzedakis, P.C., Bryant, C.L., Christanis, K., 2005. Lateglacial and Holocene vegetation history at Nisi Fen and the Boras mountains, northern Greece. The Holocene 15, 873-887.

Legendre, P., Birks, H.J.B., 2012. From classical to canonical ordination. In: Birks, H.J.B., Lotter, A.F., Juggins, S., Smol, J.P. (eds.), Tracking environmental change using lake sediments volume 5: Data handling and numerical techniques, Springer, Dordrecht, The Netherlands, pp. 201-248.

Maezumi, S.Y., Alves, D., Robinson, M., de Souza, J.G., Levis, C., Barnett, R.L., et al., 2018. The legacy of 4,500 years of polyculture agroforestry in the eastern Amazon. Nature Plants 4, 540-547.

Maniatis, Y., Kotsakis, K., Halstead, P., 2015. Paliambela Kolindrou. New dates for the Early Neolithic. AEMTH 25, 2011, pp. 140-156 (in Greek).

Maniatis, Y., Adaktylou, F., 2021. Revenia-Korinos: one of the earliest Neolithic settlements in North Greece as evidenced by radiocarbon dating. Radiocarbon 63, 1025-1051.

Marino, G., Rohling, E.J., Sangiorgi, F., Hayes, A., Casford, J.L., Lotter, A.F., et al., 2009. Early and middle Holocene in the Aegean Sea: interplay between high and low latitude climate variability. Quaternary Science Reviews 28, 3246-3262.

Marinova, E., Ntinou, M., 2018. Neolithic woodland management and land-use in south-eastern Europe: The anthracological evidence from Northern Greece and Bulgaria. Quaternary International 496, 51-67.

Masi, A., Francke, A., Pepe, C., Thienemann, M., Wagner, B., Sadori, L., 2018. Vegetation history and paleoclimate at Lake Dojran (FYROM/Greece) during the Late Glacial and Holocene. Climate of the Past 14, 351-367.

Mauri, A., de Rigo, D., Caudullo, G., 2016. *Abies alba* in Europe: distribution, habitat, usage and threats. In: San-Miguel-Ayanz, J., de Rigo, D., Caudullo, G., Houston Durrant, T., Mauri, A. (eds.), European atlas of forest tree species, Publication Office of the European Union, Luxembourg, pp. 48-49.

McWethy, D.B., Whitlock, C., Wilmshurst, J.M., McGlone, M.S., Fromont, M., Li, X., et al., 2010. Rapid landscape transformation in South Island, New Zealand, following initial Polynesian settlement. Proceedings of the National Academy of Sciences of the United States of America 107, 21343-21348.

Milner, A.M., Roucoux, K.H., Collier, R.E.L., Muller, U.C., Pross, J., Tzedakis, P.C., 2016. Vegetation responses to abrupt climatic changes during the Last Interglacial Complex (Marine Isotope Stage 5) at Tenaghi Philippon, NE Greece. Quaternary Science Reviews 154, 169-181.

Moore, P.D., Webb, J.A., Collinson, M.E., 1991. Pollen Analysis. 2nd edition. Blackwell Scientific Publications, Oxford, UK.

Morales-Molino, C., Vescovi, E., Krebs, P., Carlevaro, E., Kaltenrieder, P., Conedera, M., et al., 2015. The role of human-induced fire and sweet chestnut (*Castanea sativa* Mill.)

cultivation on the long-term landscape dynamics of the southern Swiss Alps. The Holocene 25, 482-494.

Morales-Molino, C., Tinner, W., García-Antón, M., Colombaroli, D., 2017. The historical demise of *Pinus nigra* forests in the Northern Iberian Plateau (south-western Europe). Journal of Ecology 105, 634-646.

Morales-Molino, C., Tinner, W., Perea, R., Carrión, J.S., Colombaroli, D., Valbuena-Carabaña, M., et al., 2019. Unprecedented herbivory threatens rear-edge populations of *Betula* in southwestern Eurasia. Ecology 100, e02833.

Morales-Molino, C., Steffen, M., Samartin, S., van Leeuwen, J.F.N., Hurlimann, D., Vescovi, E., Tinner, W., 2021. Long-term responses of Mediterranean mountain forests to climate change, fire and human activities in the Northern Apennines (Italy). Ecosystems 24, 1361-1377.

Morales-Molino, C., Leunda, M., Morellón, M., Gardoki, J., Ezquerra, F.J., Muñoz Sobrino, C., et al., 2022. Millennial land use explains modern high-elevation vegetation in the submediterranean mountains of Southern Europe. Journal of Biogeography 49, 1779-1792.

Ne'eman, G., Arianoutsou, M., 2021. Mediterranean pines – Adaptations to fire. In: Ne'eman, G., Osem, Y. (eds.), Pines and their mixed forest ecosystems in the Mediterranean Basin, Managing Forest Ecosystems 38, Springer, Dordrecht, The Netherlands, pp. 457-480.

Ön, Z.B., 2023. A Bayesian point change analysis re-examines the 4.2 ka BP event in southeast Europe and southwest Asia. Quaternary Science Reviews 312, 108163.

Panagiotopoulos, K., Aufgebauer, A., Schäbitz, F., Wagner, B., 2013. Vegetation and climate history of the Lake Prespa region since the Lateglacial. Quaternary International 293, 157-169.

Panagiotopoulos, K., Böhm, A., Leng, M.J., Wagner, B., Schäbitz, F., 2014. Climate variability over the last 92 ka in SW Balkans from analysis of sediments from Lake Prespa. Climate of the Past 10, 643-660.

Pasta, S., de Rigo, D., Caudullo, G., 2016. *Quercus pubescens* in Europe: distribution, habitat, usage and threats. In: San-Miguel-Ayanz, J., de Rigo, D., Caudullo, G., Houston Durrant, T., Mauri, A. (eds.), European atlas of forest tree species, Publication Office of the European Union, Luxembourg, pp. 156-157.

Peckover, E.N., Andrews, J.E., Leeder, M.R., Rowe, P.J., Marca, A., Sahy, D., Noble, S., 2019. Coupled stalagmite-alluvial fan response to the 8.2 ka event and early Holocene palaeoclimate change in Greece. Palaeogeography, Palaeoclimatology, Palaeoecology 532, 109252.

Peñalba, M.C., 1994. The history of the Holocene vegetation in northern Spain from pollen analysis. Journal of Ecology 82, 815-832.

Perring, M.P., de Frenne, P., Baeten, L., Maes, S.L., Depauw, L., Blondeel, H., et al., 2016. Global environmental change effects on ecosystems: the importance of land-use legacies. Global Change Biology 22, 1361-1371.

Pirini, C.B., Tsiripidis, I., Bergmeier, E., 2014. Steppe-like grassland vegetation in the hills around the lakes of Vegoritida and Petron, north-central Greece. Hacquetia 13, 121-169.

Pross, J., Kotthoff, U., Müller, U.C., Peyron, O., Dormoy, I., Schmiedl, G., et al., 2009. Massive perturbation in terrestrial ecosystems of the Eastern Mediterranean region associated with the 8.2 kyr B.P. climatic event. Geology 37, 887-890.

Psomiadis, D., Dotsika, E., Albanakis, K., Ghaleb, B., Hillaire-Marcel, C., 2018. Speleothem record of climatic changes in the northern Aegean region (Greece) from the Bronze Age to the collapse of the Roman Empire. Palaeogeography, Palaeoclimatology, Palaeoecology 489, 272-283.

Punt, W., et al. (eds.), 1976—2009. The Northwest European Pollen Flora, vols I-IX. Elsevier, Amsterdam, The Netherlands.

Quézel, P., Médail, F., 2003. Écologie et biogéographie des forêts du basin méditerranéen. Elsevier, Paris, France.

R Core Team, 2021. R: A language and environment for statistical computing. R Foundation for Statistical Computing, Vienna, Austria.

Reille, M. 1992. Pollen et spores d'Europe et d'Afrique du Nord. Laboratoire de botanique historique et palynologie, Marseille, France.

Reimer, P.J., Austin, W.E.N., Bard, E., Bayliss, A., Blackwell, P.G., Bronk Ramsey, C., et al., 2020. The IntCal20 Northern Hemisphere radiocarbon age calibration curve (0—55 cal kBP). Radiocarbon 62, 725-757.

Ripullone, F., Camarero, J.J., Colangelo, M., Voltas, J., 2020. Variation in the access to deep soil water pools explains tree-to-tree differences in drought-triggered dieback of Mediterranean oaks. Tree Physiology 40, 591-604.

Roberts, N., Brayshaw, D., Kuzucuoğlu, C., Pérez, R., Sadori, L., 2011. The mid-Holocene climatic transition in the Mediterranean: Causes and consequences. The Holocene 21, 3-13.

Rohling, E.J., Mayewski, P.A., Abu-Zied, R.H., Casford, J.S.L., Hayes, A., 2002. Holocene atmosphere-ocean interactions: records from Greenland and the Aegean Sea. Climate Dynamics 18, 587-593.

Rohling, E.J., Pälike, H., 2005. Centennial-scale climate cooling with a sudden cold event around 8,200 years ago. Nature 434, 975-979.

Rohling, E.J., Marino, G., Grant, K.M., Mayewski, P.A., Weninger, B., 2019. A model for archaeologically relevant Holocene climate impacts in the Aegean-Levantine region (easternmost Mediterranean). Quaternary Science Reviews 208, 38-53.

Rubio-Cuadrado, Á., Camarero, J.J., Rodríguez-Calcerrada, J., Perea, R., Gómez, C., Montes, F., Gil, L., 2021. Impact of successive spring frosts on leaf phenology and radial growth in three deciduous tree species with contrasting climate requirements in central Spain. Tree Physiology 41, 2279-2292.

Samartin, S., Heiri, O., Joos, F., Renssen, H., Franke, J., Brönnimann, S., Tinner, W., 2017. Warm Mediterranean mid-Holocene summers inferred from fossil midge assemblages. Nature Geoscience 10, 207-212.

San-Miguel-Ayanz, J., de Rigo, D., Caudullo, G., Houston Durrant, T., Mauri, A., 2016. European Atlas of Forest Tree Species. Publications Office of the European Union, Luxembourg.

Sánchez de Dios, R., Gómez, C., Aulló, I., Cañellas, I., Gea-Izquierdo, G., Montes, F., et al., 2021. *Fagus sylvatica* L., peripheral populations in the Mediterranean Iberian Peninsula: climatic or anthropic relicts? Ecosystems 24, 211-226.

Senn, C., Tinner, W., Felde, V.A., Gobet, E., van Leeuwen, J.F.N., Morales-Molino, C., 2022. Modern pollen-vegetation-plant diversity relationships across large environmental gradients in northern Greece. The Holocene 32, 159-173.

Skoulikidis, N.T., Bertahas, I., Koussouris, T., 1998. The environmental state of freshwater resources in Greece (rivers and lakes). Environmental Geology 36, 1-17.

Šmilauer, P., Lepš, J., 2014. Multivariate analysis of ecological data using Canoco 5, 2nd edition. Cambridge University Press, Cambridge, United Kingdom.

Stefanova, I., Ammann, B., 2003. Lateglacial and Holocene vegetation belts in the Pirin Mountains (southwestern Bulgaria). The Holocene 13, 97-107.

Stefanova, I., Atanassova, J., Delcheva, M., Wright, H.E., 2006. Chronological framework for the Lateglacial pollen and macrofossil sequence in the Pirin Mountains, Bulgaria: Lake Besbog and Lake Kremensko-5. The Holocene 16, 877-892.

Stockmarr, J.,1971. Tablets with spores used in absolute pollen analysis. Pollen et spores 13, 615-621.

Sugita, S., 1994. Pollen representation of vegetation in Quaternary sediments: theory and method in patchy vegetation. Journal of Ecology 82, 881-897.

Swetnam, T.W., Allen, C.D., Betancourt, J.L., 1999. Applied historical ecology: using the past to manage for the future. Ecological Applications 9, 1189-1206.

Szidat, S., Salazar, G.A., Vogel, E., Battaglia, M., Wacker, L., Synal, H.-A., Türler, A., 2014. ^{14}C analysis and sample preparation at the new Bern Laboratory for the Analysis of Radiocarbon with AMS (LARA). Radiocarbon 56, 561-566.

Tapias, R., Climent, J., Pardos, J.A., Gil, L., 2004. Life histories of Mediterranean pines. Plant Ecology 171, 53-68.

ter Braak, C.J.F., Šmilauer, P., 2012. Canoco reference manual and user's guide: software for ordination, version 5.0. Microcomputer power, Ithaca, NY, USA.

Tichý, L., Axmanová, I., Dengler, J., Guarino, R., Jansen, F., Midolo, G., et al., 2023. Ellenberg-type indicator values for European vascular plant species. Journal of Vegetation Science 34, e13168.

Tinner, W., Conedera, M., Ammann, B., Gaggeler, H.W., Gedye, S., Jones, R., Sagesser, B., 1998. Pollen and charcoal in lake sediments compared with historically documented forest fires in southern Switzerland since AD 1920. The Holocene 8, 31-42.

Tinner, W., Hubschmid, P., Wehrli, M., Ammann, B., Conedera, M., 1999. Long-term forest fire ecology and dynamics in southern Switzerland. Journal of Ecology 87, 273-289.

Tinner, W., Hu, F.S., 2003. Size parameters, size-class distribution and area-number relationship of microscopic charcoal: Relevance for fire reconstructions. The Holocene 13, 499-505.

Tinner, W., Lotter, A.F., 2006. Holocene expansions of *Fagus sylvatica* and *Abies alba* in Central Europe: where are we after eight decades of debate? Quaternary Science Reviews 25, 526-549.

Tinner, W., Colombaroli, D., Heiri, O., Henne, P.D., Steinacher, M., Untenecker, J., et al., 2013. The past ecology of *Abies alba* provides new perspectives on future responses of silver fir forests to global warming. Ecological Monographs 83, 419-439.

Tonkov, S., 2021. The postglacial vegetation history of southwestern Bulgaria. A palaeoecological approach. Pensoft Publishers, Sofia, Bulgaria.

Tóth, M., Magyari, E.K., Buczkó, K., Braun, M., Panagiotopoulos, K., Heiri, O., 2015. Chironomid-inferred Holocene temperature changes in the South Carpathians (Romania). The Holocene 25, 569-582.

Trautmann, W., 1953. Zur Unterscheidung fossiler Spaltöffnungen der mitteleuropäischen Coniferen. Flora 140, 523-533.

Triantaphyllou, M.V., Gogou, A., Dimiza, M.D., Kostopoulou, S., Parinos, C., Roussakis, et al., 2016. Holocene Climatic Optimum centennial-scale paleoceanography in the NE Aegean (Mediterranean Sea). Geo-Marine Letters 36, 51-66.

Tzedakis, P.C., 1993. Long-term tree populations in northwest Greece through multiple Quaternary climatic cycles. Nature 364, 437-440.

Tzedakis, P.C., Hooghiemstra, H., Pälike, H., 2006. The last 1.35 million years at Tenaghi Philippon: revised chronostratigraphy and long-term vegetation trends. Quaternary Science Reviews 25, 3416-3430.

van Geel, B., Buurman, J., Brinkkemper, O., Schelvis, J., Aptroot, A., van Reenen, G., Hakbijl, T., 2003. Environmental reconstruction of a Roman Period settlement site in Uitgeest (The Netherlands), with special reference to coprophilous fungi. Journal of Archaeological Science 30, 873-883.

van Geel, B., Aptroot, A., 2006. Fossil ascomycetes in Quaternary deposits. Nova Hedwigia 82, 313-329.

Vescovi, E., Kaltenrieder, P., Tinner, W., 2010. Late-Glacial and Holocene vegetation history of Pavullo nel Frignano (Northern Apennines, Italy). Review of Palaeobotany and Palynology 160, 32-45.

Vilà-Cabrera, A., Astigarraga, J., Jump, A.S., Zavala, M.A., Seijo, F., Sperlich, D., Ruiz-Benito, P., 2023. Anthropogenic land-use legacies underpin climate change-related risks to forest ecosystems. Trends in Plant Science 28, 1132-1143.

Wagner, B., Lotter, A.F., Nowaczyk, N., Reed, J.M., Schwalb, A., Sulpizio, R., et al., 2009. A 40,000-year record of environmental change from ancient Lake Ohrid (Albania and Macedonia). Journal of Paleolimnology 41, 407-430.

Weiberg, E., Bevan, A., Kouli, K., Katsianis, M., Woodbridge, J., Bonnier, A., et al., 2019. Long-term trends of land use and demography in Greece: A comparative study. The Holocene 29, 742-760.

Whitlock, C., Colombaroli, D., Conedera, M., Tinner, W., 2018. Land-use history as a guide for forest conservation and management. Conservation Biology 32, 84-97.

Willis, K.J., 1992a. The late Quaternary vegetational history of northwest Greece. I. Lake Gramousti. New Phytologist 121, 101-117.

Willis, K.J., 1992b. The late Quaternary vegetational history of northwest Greece. II. Rezina marsh. New Phytologist 121, 119-138.

Willis, K.J., 1994. The vegetational history of the Balkans. Quaternary Science Reviews 13, 769-788.

Zhang, X.S., Reed, J.M., Lacey, J.H., Francke, A., Leng, M.J., Levkov, Z., Wagner, B., 2016. Complexity of diatom response to Lateglacial and Holocene climate and environmental change in ancient, deep and oligotrophic Lake Ohrid (Macedonia and Albania). Biogeosciences 13, 1351-1365.

Table 1. Radiocarbon dates of the Limni Vegoritis sedimentary sequence. Radiocarbon dates were calibrated using the R package 'clam' version 2.3.9 (Blaauw, 2010) and the IntCal20 calibration curve (Reimer et al., 2020). Calibrated ages have been rounded to the nearest decade.

Laboratory code	Depth (cm)	Material dated	Radiocarbon age (^{14}C BP)	Calibrated age (cal. BP, 95% CI)	Age in diagram (cal. BP)
BE-6342	119	Branch (twig)	390 ± 20	330—500	460
BE-16305	256—264	Leaf fragments	1890 ± 65	1630—1980	1620
BE-17475	370—374	*Carex* fruit, terrestrial plant remains	1690 ± 65	1410—1710	1700
BE-6343	433—435	Branch (twig)	2260 ± 20	2160—2340	2330
BE-17473	466—468	*Pinus* needle fragments, dwarf shoot, bud scale	2980 ± 85	2930—3370	3040
BE-6344	512	Branch (twig)	3680 ± 20	3930—4090	3970
BE-16304	540—536	Seed, leaf fragments	7040 ± 35	*Rejected*	*Rejected*
BE-16303	618—622	Leaf fragments, *Pinus* bud scale, charred leaves, *Carex* fruit	4580 ± 85	4970—5550	5330
BE-21477	656—658	Bud scales, (charred) leaf fragments, *Pinus* needle fragment, anther	5130 ± 80	5660—6170	5960
BE-6345	715	Bark	6300 ± 25	7160—7270	7170
BE-16302	776—780	Leaf fragments, charred leaves	7240 ± 95	7870—8320	8120
BE-16301	826—828	Leaf fragments, *Pinus* seed wing	7960 ± 100	8550—9080	8800

Figure 1. Top left. Limni Vegoritis and its surroundings seen from the Voras Mountains, with the location of the coring site in the small basin, a relatively shallow embayment on the northeast corner of the lake. **Top right.** Location of Limni Vegoritis in Northern Greece and other regional palaeoecological and palaeoclimatic records mentioned in the text: 1 Limni Vegoritis (Bottema, 1982; this study), Nisi Fen (Lawson et al., 2005) and Edessa (Bottema, 1974); 2 Limni Zazari (Gassner et al., 2020) and Limni Chimaditis (Bottema, 1974); 3 Limni Orestiás (Bottema, 1974; Kouli and Dermitzakis, 2010); 4 Lake Ohrid (Wagner et al., 2009; Brechbühl et al., 2024), Lake Prespa (Panagiotopoulos et al., 2013) and Lake Maliq (Denèfle et al., 2000); 5 Lake Gramousti (Willis, 1992a), Rezina marsh (Willis, 1992b) and Ioannina basin (Lawson et al., 2004); 6 Lake Dojran (Masi et al., 2018); 7 Tenaghi Philippon-Dikili Tash (Pross et al., 2009; Glais et al., 2016, 2017); 8 Skala Marion Cave (Psomiadis et al., 2018); 9 GeoTü SL152 (Kotthoff et al., 2008); 10 SL21 (Marino et al., 2009); 11 Limnon Cave (Peckover et al., 2019); 12 Kapsia Cave (Finné et al., 2014); 13 LC21 (Rohling et al., 2002; Marino et al., 2009); 14 Mavri Trypa Cave (Finné et al., 2017); 15 Sofular Cave (Fleitmann et al., 2009; Göktürk et al., 2011); 16 Lake Brazi (Tóth et al., 2015). **Bottom.** Detailed map of Northern Greece showing the location of Limni Vegoritis and the main pollen sites discussed in the text.

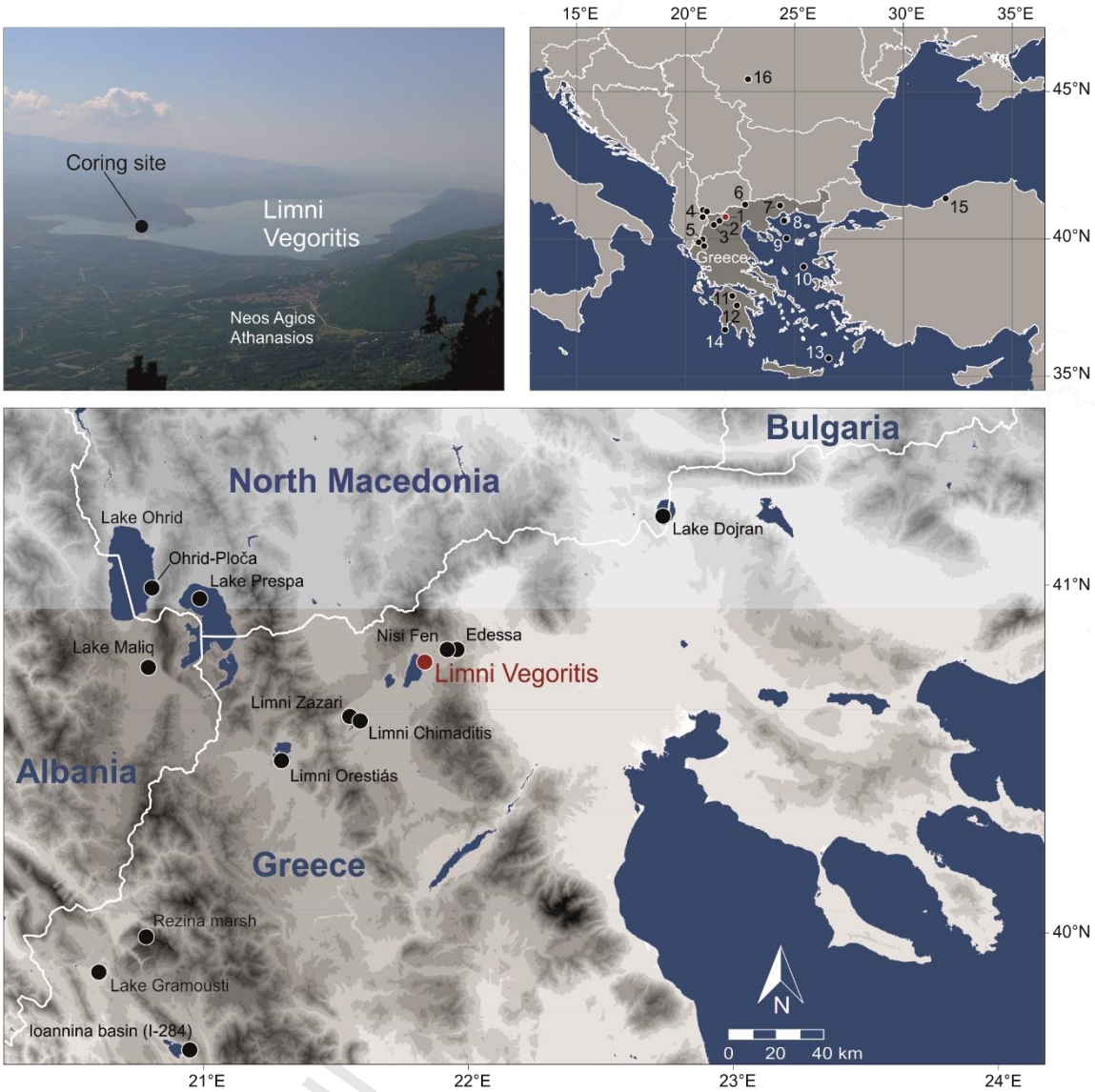
Coring site
Limni Vegoritis
Neos Agios Athanasios
15°E
20°E
25°E
30°E
35°E
45°N
40°N
35°N
Greece
Bulgaria
North Macedonia
Lake Ohrid
Ohrid-Ploča
Lake Prespa
Lake Dojran
41°N
Lake Maliq
Nisi Fen
Edessa
Limni Vegoritis
Limni Zazari
Limni Chimaditis
Albania
Limni Orestiás
Greece
Rezina marsh
Lake Gramousti
Ioannina basin (I-284)
N
0 20 40 km
21°E
22°E
23°E
24°E

Figure 2. From left to right: Lithostratigraphy, age-depth model, sediment accumulation rate and total pollen concentration (terrestrial plants) of the Limni Vegoritis sedimentary record. A section of the sequence consisting of turbidites and inorganic deposits (clay and silt) has been considered as associated with a 'rapid deposition episode' and was therefore excluded from the age-depth model. The age-depth relationship (black solid line) has been modelled fitting a smoothing spline (smoothing parameter = 0.25) to the accepted radiocarbon dates with 'clam' (Blaauw, 2010). The grey envelope delimits the 95% confidence interval (based on 10,000 iterations).

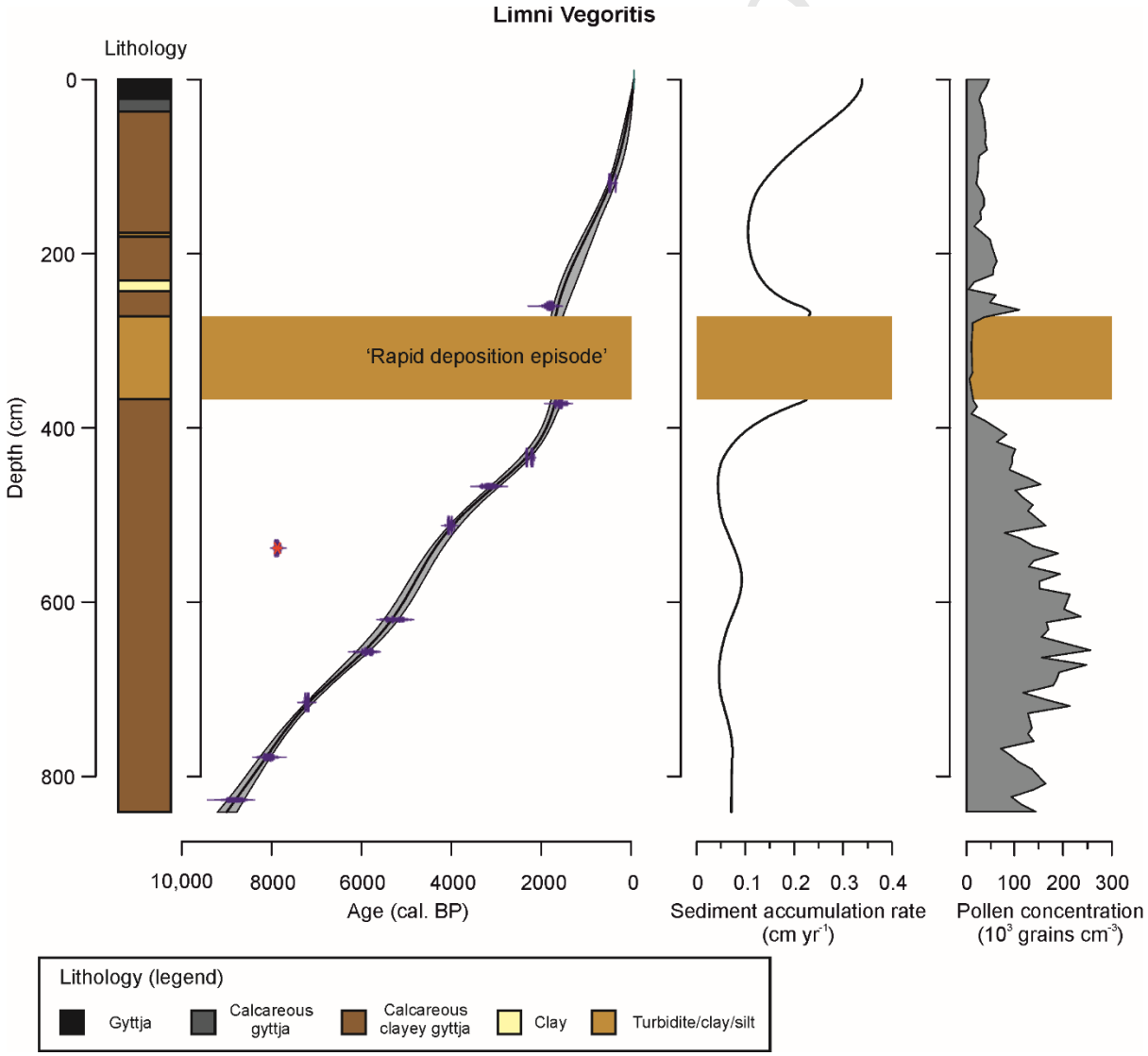

Figure 3. Pollen diagram of Limni Vegoritis: selected trees and shrubs (abundances expressed as percentages of the terrestrial pollen sum), plus microscopic charcoal and *Sporormiella* type (influx values). Hollow curves represent 10× exaggeration. Dots represent presence. LPAZ: statistically significant local pollen assemblage zones. The 'rapid deposition episode' is shaded in grey.

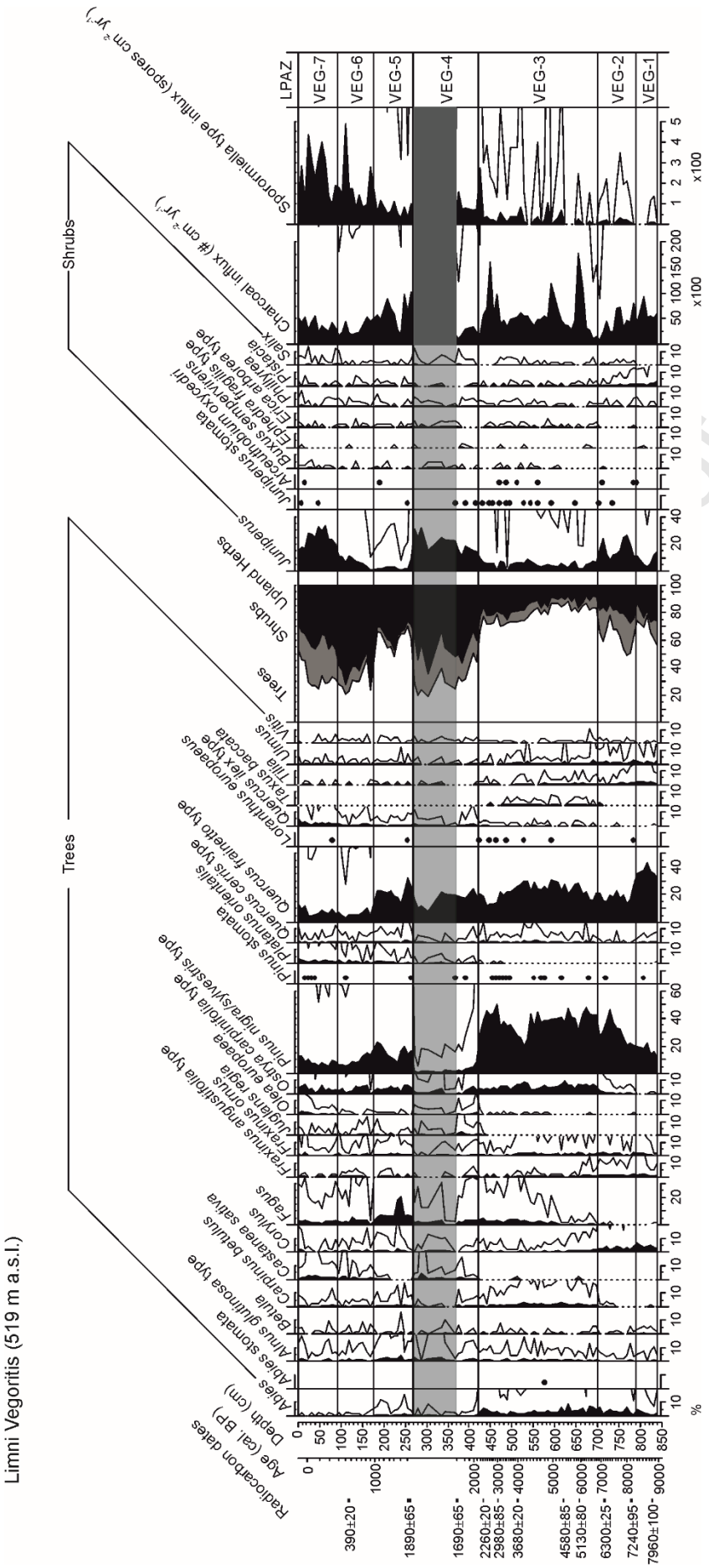
Limni Vegoritis (519 m a.s.l.)
Radiocarbon dates
Age (cal. BP)
Depth (cm)
Trees
Shrubs
Abies
Abies stomata
Alnus glutinosa type
Betula
Carpinus betulus
Castanea sativa
Corylus
Fagus
Fraxinus angustifolia type
Fraxinus ornus
Juglans regia
Olea europaea
Ostrya carpinifolia type
Pinus nigra/sylvestris type
Pinus stomata
Platanus orientalis
Quercus cerris type
Quercus frainetto type
Loranthus europaeus
Quercus ilex type
Taxus baccata
Tilia
Ulmus
Vitis
Trees
Shrubs
Upland Herbs
Juniperus
Juniperus stomata
Arceuthobium oxycedri
Buxus sempervirens
Ephedra fragilis type
Erica arborea type
Phillyrea
Pistacia
Salix
Charcoal influx (# cm⁻² yr⁻¹)
Sporormiella type influx (spores cm⁻² yr⁻¹)
LPAZ
VEG-7
VEG-6
VEG-5
VEG-4
VEG-3
VEG-2
VEG-1
390±20
1890±65
1690±65
2260±20
2980±85
3680±20
4580±85
5130±80
6300±25
7240±95
7960±100
x100
x100

Figure 4. Percentage pollen diagram of Limni Vegoritis: selected upland herbs, ferns, and wetland plants. Hollow curves represent 10× exaggeration. LPAZ: statistically significant local pollen assemblage zones. The ‘rapid deposition episode’ is shaded in grey.

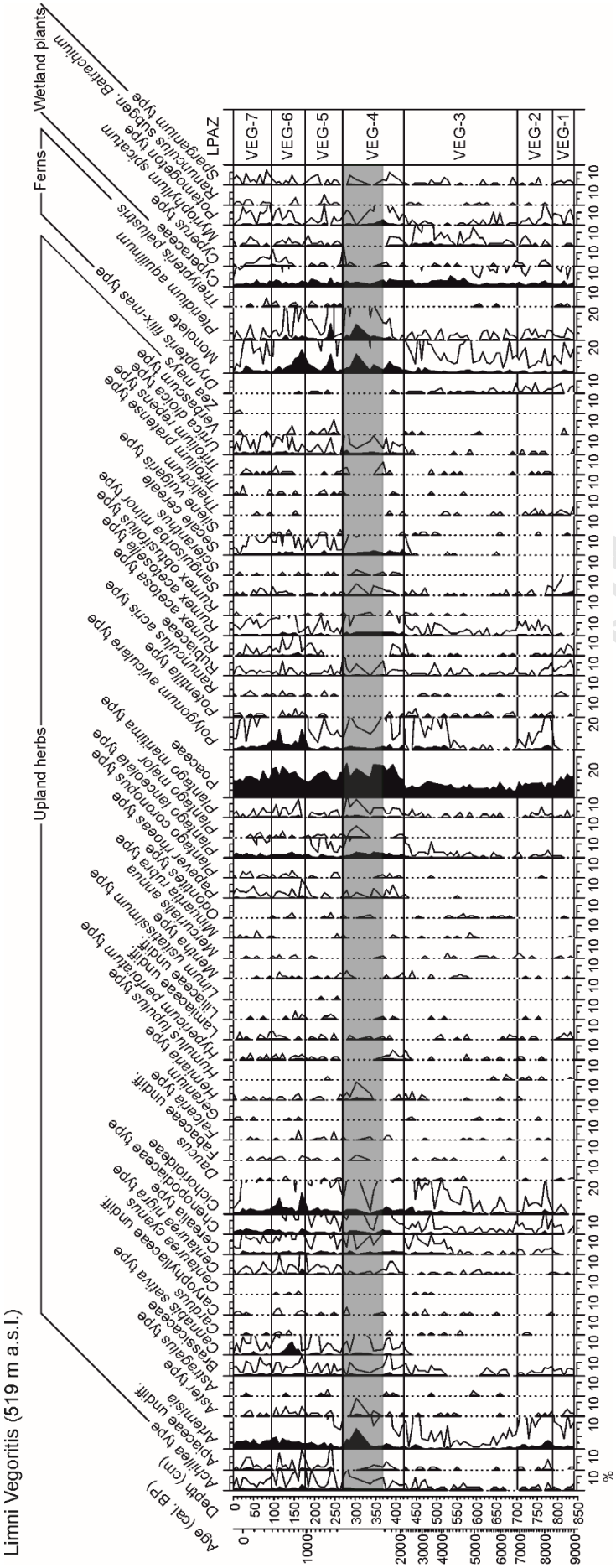
Limni Vegoritis (519 m a.s.l.)
Age (cal. BP)
Depth (cm)
Upland herbs
Ferns
Wetland plants
LPAZ
VEG-7
VEG-6
VEG-5
VEG-4
VEG-3
VEG-2
VEG-1
%

Figure 5. Vegetation dynamics at Limni Vegoritis and its drivers. **(a)** Main cultural periods in Northern Greece (delimited by dotted lines). 'Ancient Greece' includes the time from the Iron Age to the Hellenic Period as in Roberts et al. (2011). **(b)** $\delta^{13}C$ curve of the Sofular Cave speleothems (northern Anatolia), a proxy for regional moisture conditions during spring-summer-autumn (Fleitmann et al., 2009; Göktürk et al., 2011). **(c)** July air temperature reconstruction at the elevation of Limni Vegoritis based on the chironomid record of Lake Brazi (Romanian Carpathians; Tóth et al., 2015). A lapse rate of 0.65°C/100 m was applied in the calculation. **(d)** Microscopic charcoal influx from Limni Vegoritis as a proxy for extra-local to regional fire occurrence. **(e)** *Sporormiella* t. spore influx from Limni Vegoritis as a proxy for pastoralism intensity. **(f)** Pollen abundance (%) of the main herbaceous crops and cultivated trees found in the Limni Vegoritis record. **(g)** Pollen abundance (%) of the main apophytes of the Limni Vegoritis record. **(h)** Main pollen diagram (%) that reflects changes in vegetation composition. **(i)** Pollen abundance (%) of the main woody taxa of the Limni Vegoritis record. Dots denote the presence of conifer stomata. **(j)** Statistically significant local pollen assemblage zones of the Limni Vegoritis pollen record (shaded in grey and white). The '8.2 ka event' (delimited according to Rohling and Pälike, 2005) and the '4.2 ka event' (delimited according to Bini et al., 2019) have been shaded in purple.

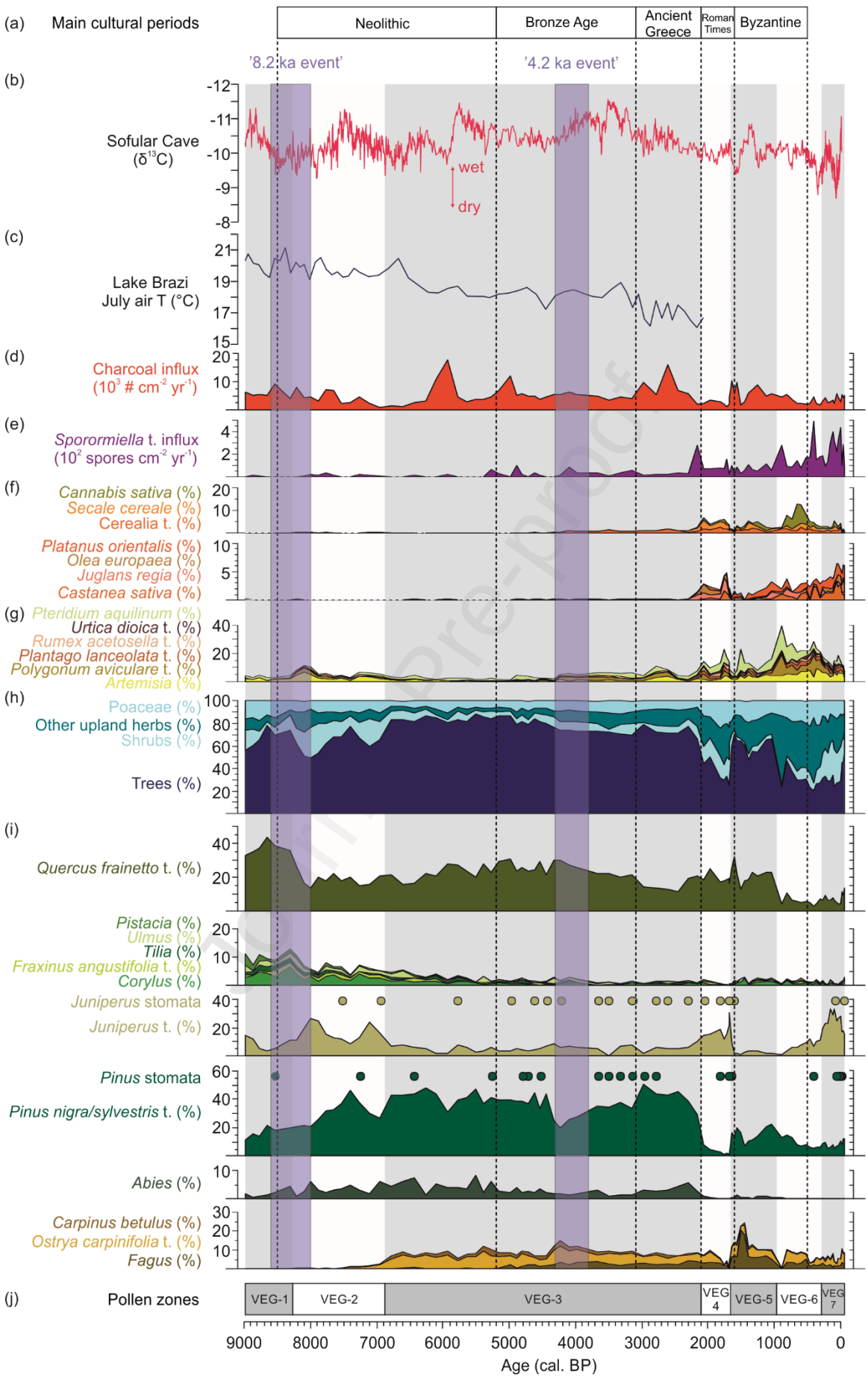
(a) Main cultural periods
Neolithic
Bronze Age
Ancient Greece
Roman Times
Byzantine
'8.2 ka event'
'4.2 ka event'
(b)
Sofular Cave (δ13C)
wet
dry
(c)
Lake Brazi July air T (°C)
(d)
Charcoal influx (10³ # cm⁻² yr⁻¹)
(e)
Sporormiella t. influx (10² spores cm⁻² yr⁻¹)
(f)
Cannabis sativa (%)
Secale cereale (%)
Cerealia t. (%)
Platanus orientalis (%)
Olea europaea (%)
Juglans regia (%)
Castanea sativa (%)
(g)
Pteridium aquilinum (%)
Urtica dioica t. (%)
Rumex acetosella t. (%)
Plantago lanceolata t. (%)
Polygonum aviculare t. (%)
Artemisia (%)
(h)
Poaceae (%)
Other upland herbs (%)
Shrubs (%)
Trees (%)
(i)
Quercus frainetto t. (%)
Pistacia (%)
Ulmus (%)
Tilia (%)
Fraxinus angustifolia t. (%)
Corylus (%)
Juniperus stomata
Juniperus t. (%)
Pinus stomata
Pinus nigra/sylvestris t. (%)
Abies (%)
Carpinus betulus (%)
Ostrya carpinifolia t. (%)
Fagus (%)
(j) Pollen zones
VEG-1
VEG-2
VEG-3
VEG 4
VEG-5
VEG-6
VEG 7
9000
8000
7000
6000
5000
4000
3000
2000
1000
0
Age (cal. BP)

Figure 6. Ordination biplots of the Limni Vegoritis palaeoecological record. **(a)** Principal component analysis (PCA) biplot representing species loadings (arrows) and sample scores (symbols) on the first two axes. Axis 1 and 2 explain 41.5% and 12.6% of the variation in the pollen dataset, respectively. The different symbols denote the statistically significant local pollen assemblage zones. **(b)** Redundancy analysis (RDA) biplot depicting the relationship between microscopic charcoal influx (proxy for fire occurrence) and *Sporormiella* t. influx (proxy for pastoral farming), which are the environmental variables selected, and the relative abundances of the main pollen types, which are the response variables. The environmental variables explain together the 21.9% of the variation in the pollen dataset (microscopic charcoal influx = 1.4%, *Sporormiella* t. influx = 17.6%, shared = 2.9%).

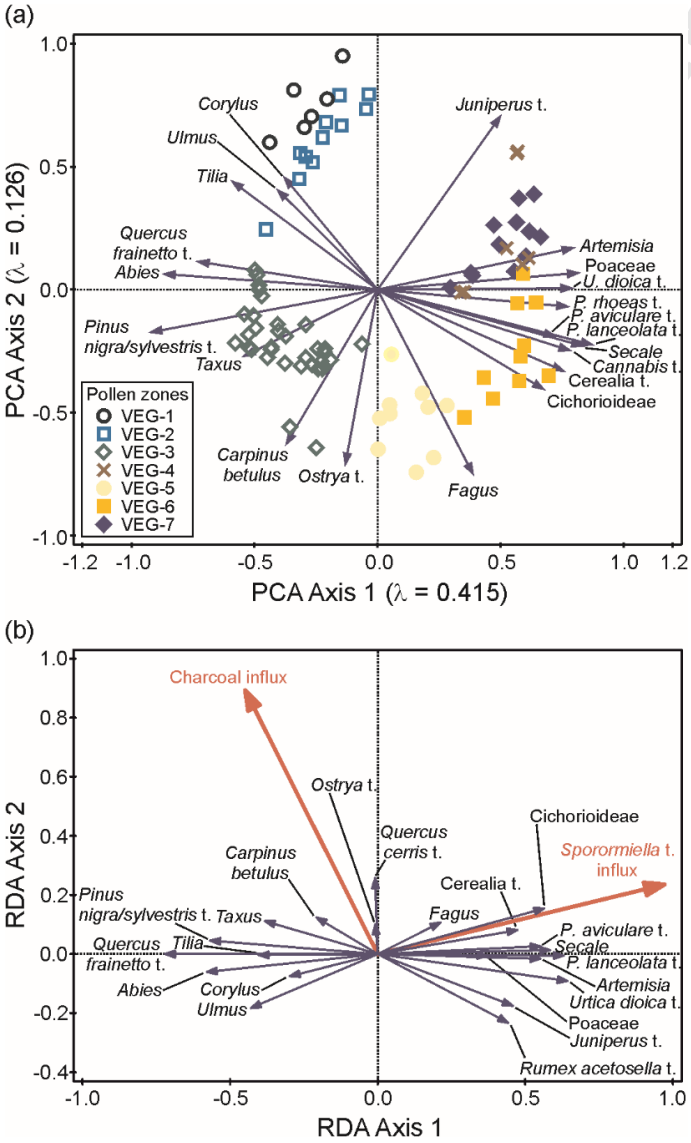

Declaration of interests

☒The authors declare that they have no known competing financial interests or personal relationships that could have appeared to influence the work reported in this paper.

☐The authors declare the following financial interests/personal relationships which may be considered as potential competing interests:

Graphical abstract

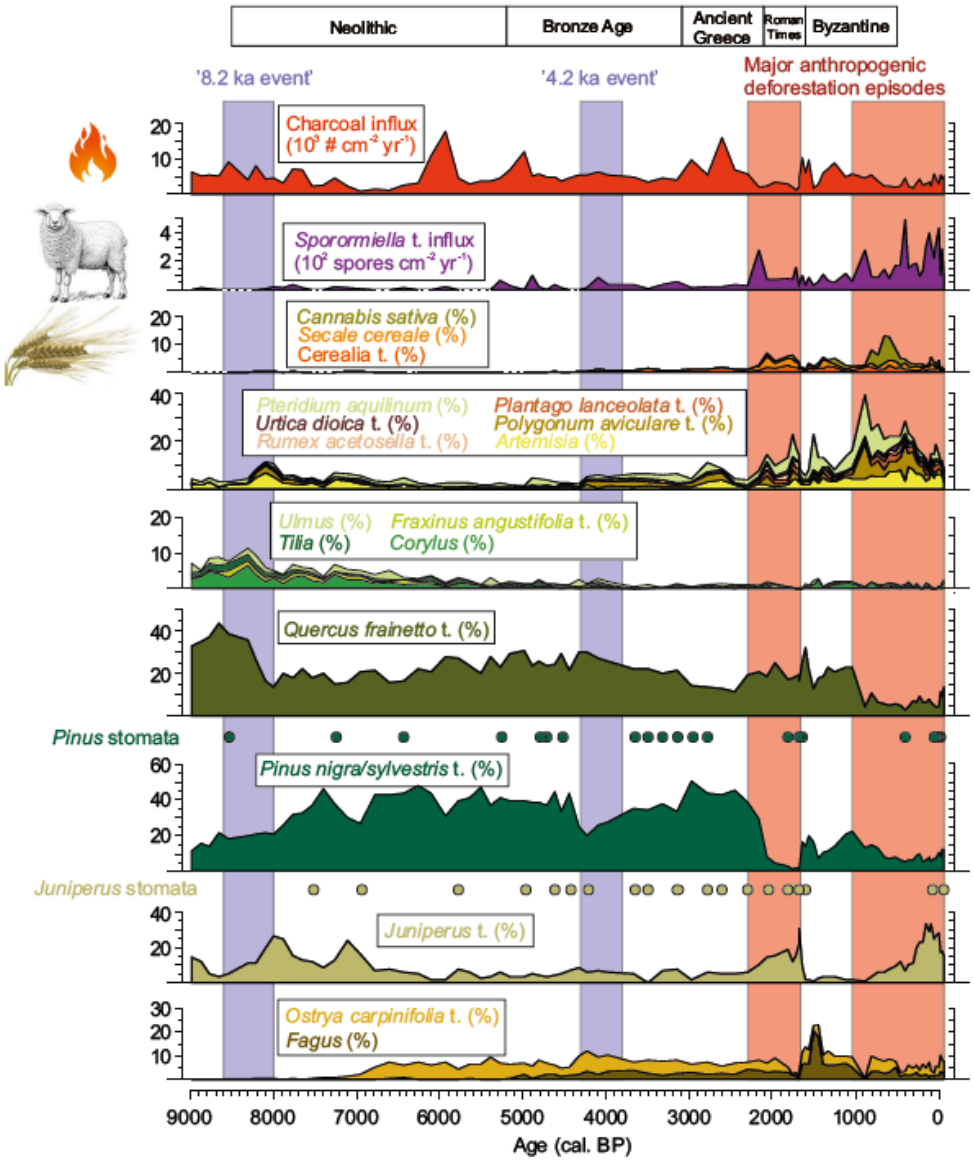

Highlights

We investigated the legacy of past land use on the current landscapes of N Greece

We assessed the impact of 9000 years of climate variability on vegetation dynamics

We studied the sediment record of Limni Vegoritis using palaeoecological tools

The 8.2 ka event triggered a major vegetation shift, namely woodland opening

Today's deforested landscape originated ~2000 years ago with pinewood extirpation

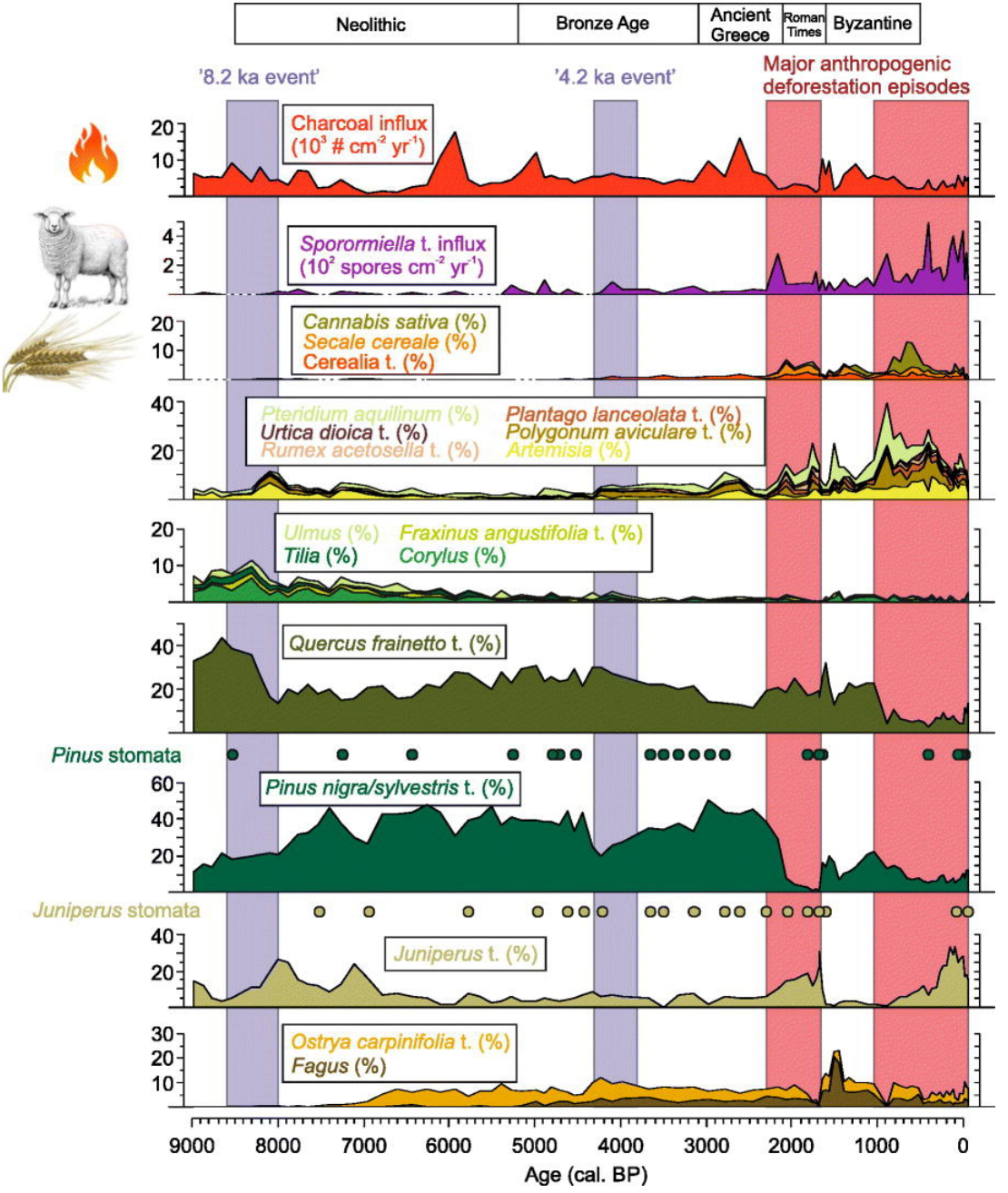

Graphics Abstract

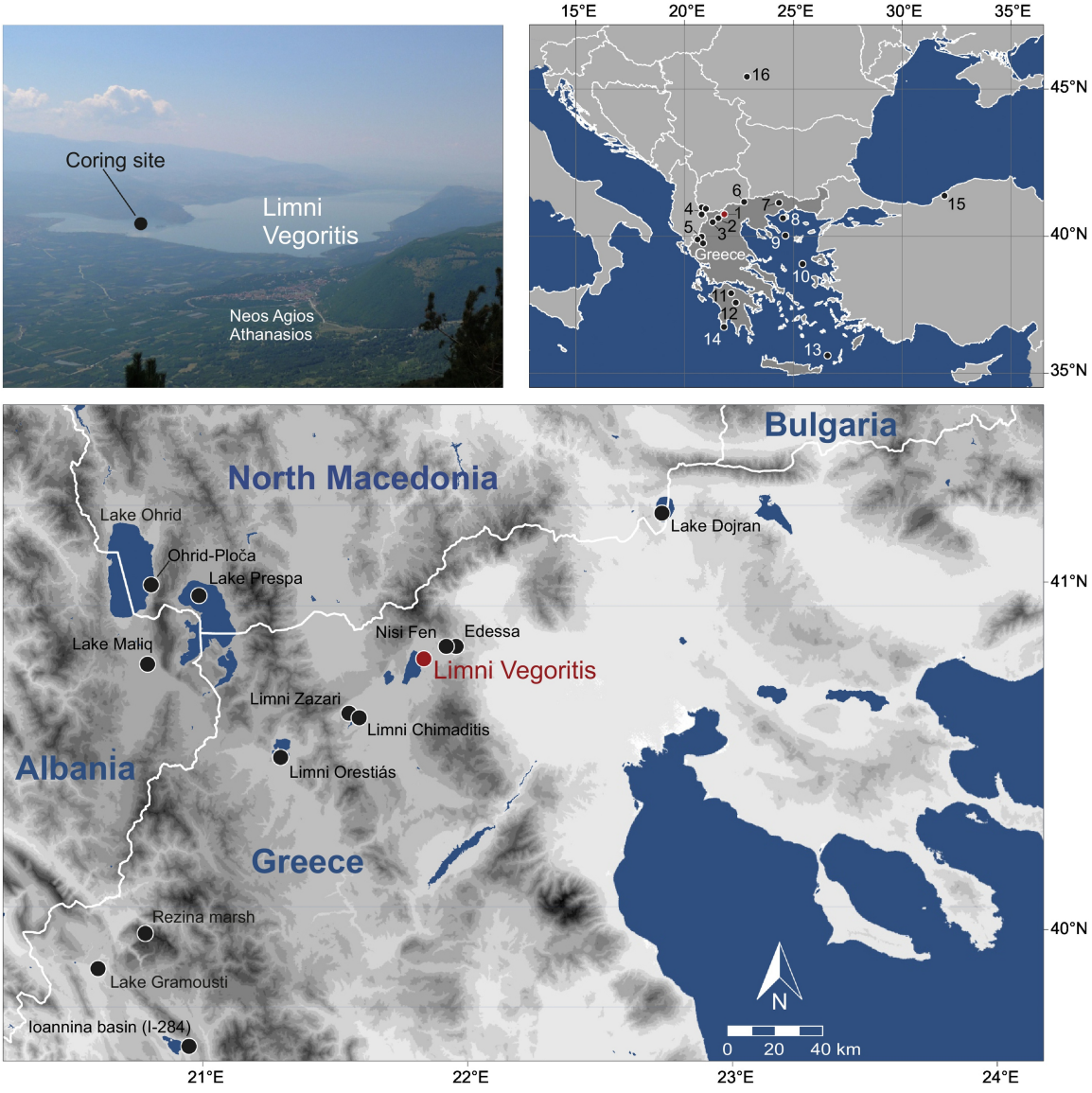
Coring site
Limni
Vegoritis
Neos Agios
Athanasios
15°E
20°E
25°E
30°E
35°E
45°N
40°N
35°N
16
6
7
4
1
8
5
2
3
9
15
Greece
10
11
12
14
13
Bulgaria
North Macedonia
Lake Ohrid
Ohrid-Ploča
Lake Prespa
Lake Dojran
41°N
Nisi Fen
Edessa
Lake Maliq
Limni Vegoritis
Limni Zazari
Limni Chimaditis
Albania
Limni Orestiás
Greece
Rezina marsh
40°N
Lake Gramousti
Ioannina basin (I-284)
N
0
20
40 km
21°E
22°E
23°E
24°E

Figure 1

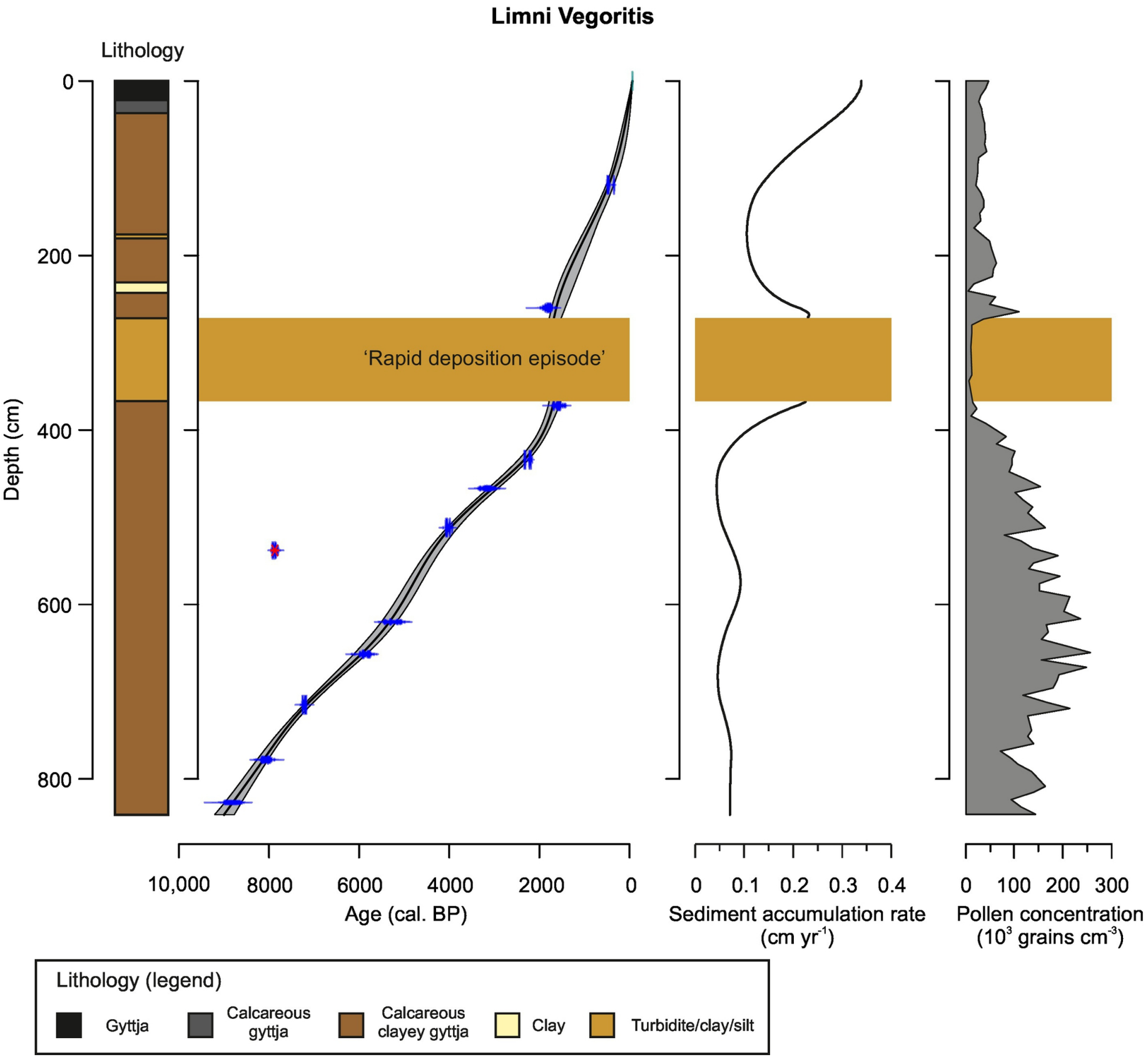
Limni Vegoritis
Lithology
Depth (cm)
0
200
400
600
800
'Rapid deposition episode'
10,000
8000
6000
4000
2000
0
Age (cal. BP)
0
0.1
0.2
0.3
0.4
Sediment accumulation rate
(cm yr-1)
0
100
200
300
Pollen concentration
(10^3 grains cm^-3)
Lithology (legend)
Gyttja
Calcareous gyttja
Calcareous clayey gyttja
Clay
Turbidite/clay/silt

Figure 2

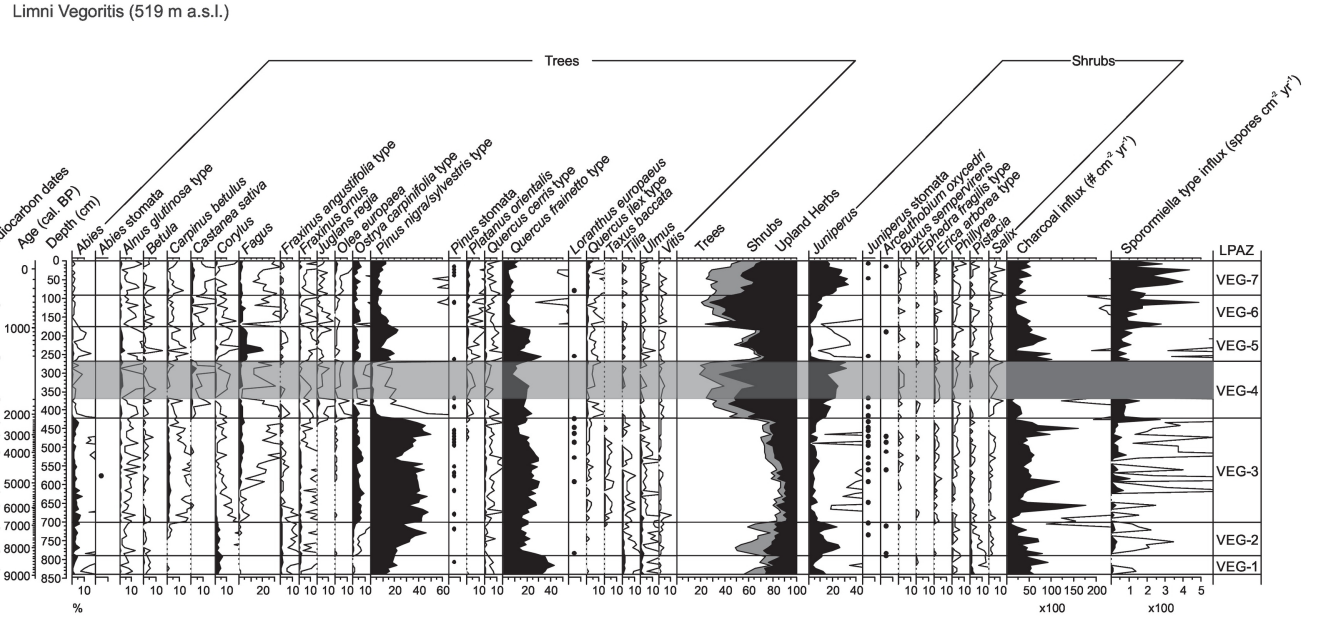
Limni Vegoritis (519 m a.s.l.)
Trees
Shrubs
Radiocarbon dates
Age (cal. BP)
Depth (cm)
Abies
Abies stomata
Alnus glutinosa type
Betula
Carpinus betulus
Castanea sativa
Corylus
Fagus
Fraxinus angustifolia type
Fraxinus ornus
Juglans regia
Olea europaea
Ostrya carpinifolia type
Pinus nigra/sylvestris type
Pinus stomata
Platanus orientalis
Quercus cerris type
Quercus frainetto type
Loranthus europaeus
Quercus ilex type
Taxus baccata
Tilia
Ulmus
Vitis
Trees
Shrubs
Upland Herbs
Juniperus
Juniperus stomata
Arceuthobium oxycedri
Buxus sempervirens
Ephedra fragilis type
Erica arborea type
Phillyrea
Pistacia
Salix
Charcoal influx (# cm-2 yr-1)
Sporormiella type influx (spores cm-2 yr-1)
LPAZ
VEG-7
VEG-6
VEG-5
VEG-4
VEG-3
VEG-2
VEG-1
390±20
1890±65
1690±65
2260±20
2980±85
3680±20
4580±85
5130±80
6300±25
7240±95
7960±100
%
x100
x100

Figure 3

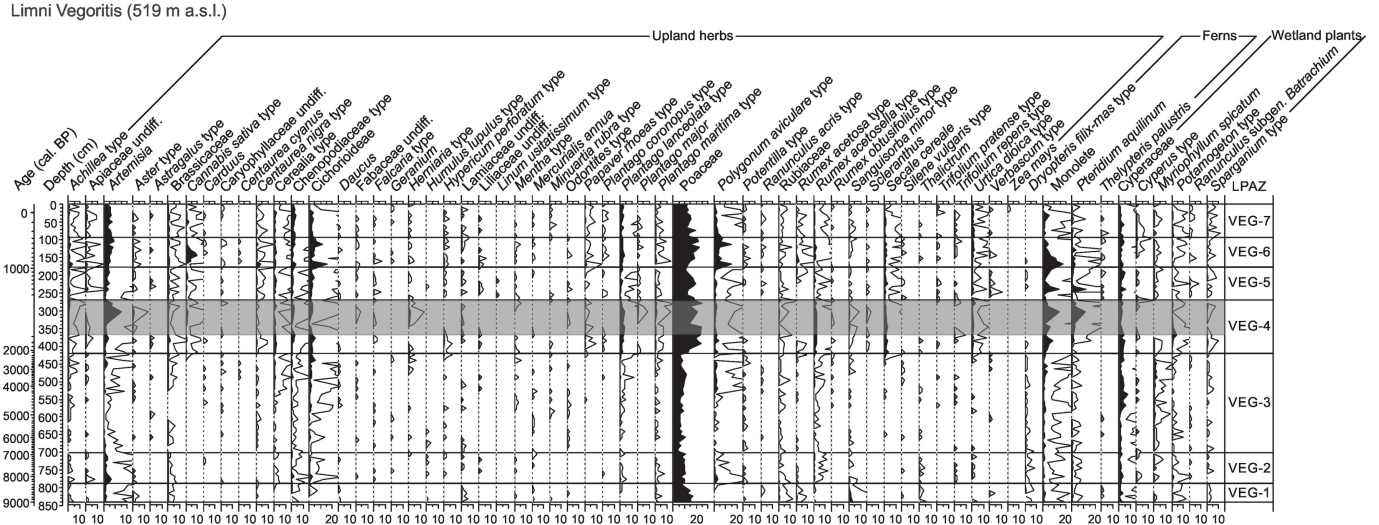
Limni Vegoritis (519 m a.s.l.)
Upland herbs
Ferns
Wetland plants
Age (cal. BP)
Depth (cm)
Achillea type
Apiaceae undiff.
Artemisia
Aster type
Astragalus type
Brassicaceae
Cannabis sativa type
Carduus
Caryophyllaceae undiff.
Centaurea cyanus
Centaurea nigra type
Cerealia type
Chenopodiaceae type
Cichorioideae
Daucus
Fabaceae undiff.
Falcaria type
Geranium
Herniaria type
Humulus lupulus type
Hypericum perforatum type
Lamiaceae undiff.
Liliaceae undiff.
Linum usitatissimum type
Mentha type
Mercurialis annua
Minuartia rubra type
Odontites type
Papaver rhoeas type
Plantago coronopus type
Plantago lanceolata type
Plantago major
Plantago maritima type
Poaceae
Polygonum aviculare type
Potentilla type
Ranunculus acris type
Rubiaceae
Rumex acetosa type
Rumex acetosella type
Rumex obtusifolius type
Sanguisorba minor type
Scleranthus
Secale cereale
Silene vulgaris type
Thalictrum
Trifolium pratense type
Trifolium repens type
Urtica dioica type
Verbascum type
Zea mays
Dryopteris filix-mas type
Monolete
Pteridium aquilinum
Thelypteris palustris
Cyperaceae
Cyperus type
Myriophyllum spicatum
Potamogeton type
Ranunculus subgen. Batrachium
Sparganium type
LPAZ
VEG-7
VEG-6
VEG-5
VEG-4
VEG-3
VEG-2
VEG-1
%

Figure 4

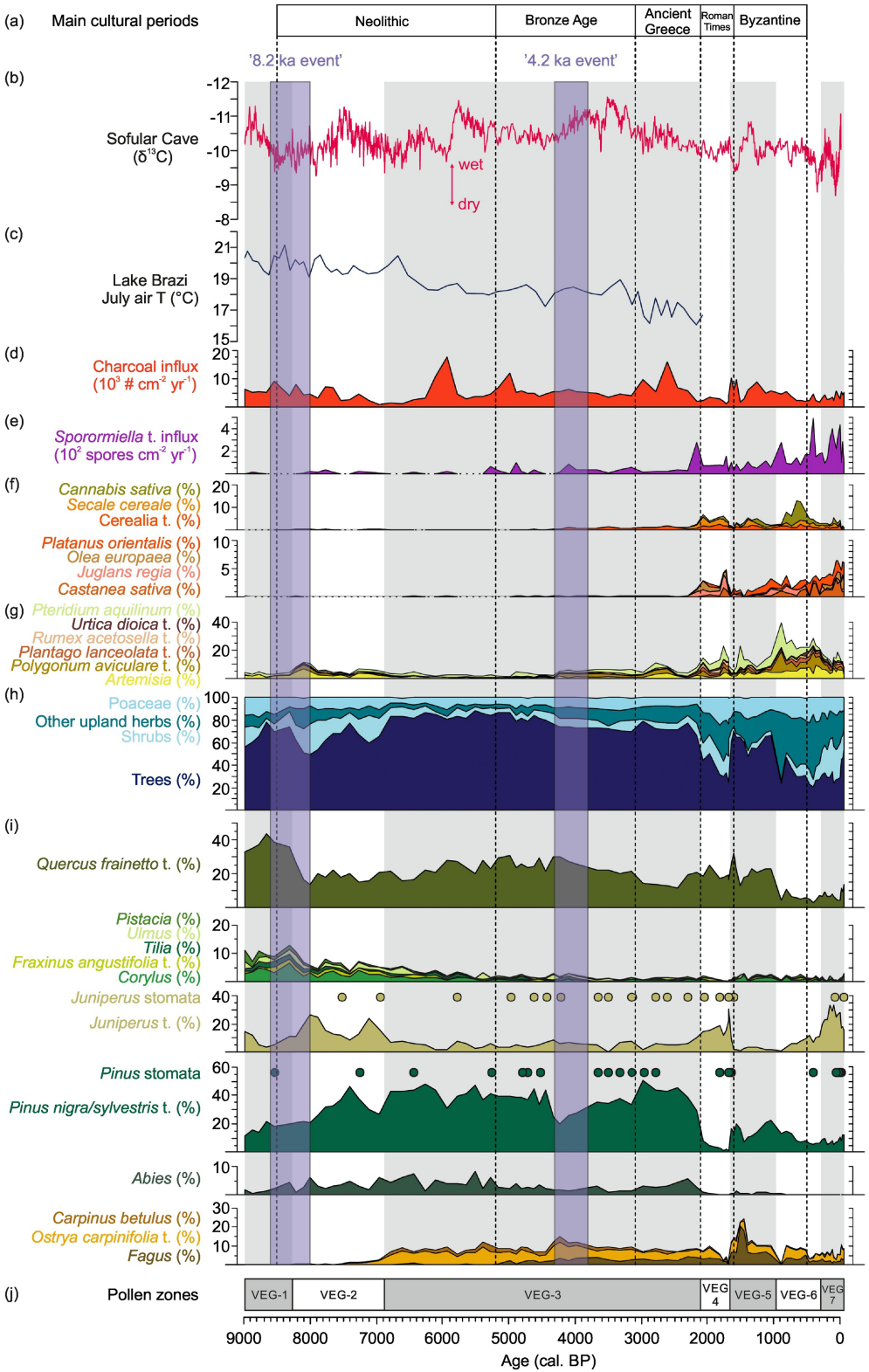
(a) Main cultural periods
Neolithic
Bronze Age
Ancient Greece
Roman Times
Byzantine
'8.2 ka event'
'4.2 ka event'
(b)
Sofular Cave (δ13C)
wet
dry
(c)
Lake Brazi July air T (°C)
(d)
Charcoal influx (10³ # cm⁻² yr⁻¹)
(e)
Sporormiella t. influx (10² spores cm⁻² yr⁻¹)
(f)
Cannabis sativa (%)
Secale cereale (%)
Cerealia t. (%)
Platanus orientalis (%)
Olea europaea (%)
Juglans regia (%)
Castanea sativa (%)
(g)
Pteridium aquilinum (%)
Urtica dioica t. (%)
Rumex acetosella t. (%)
Plantago lanceolata t. (%)
Polygonum aviculare t. (%)
Artemisia (%)
(h)
Poaceae (%)
Other upland herbs (%)
Shrubs (%)
Trees (%)
(i)
Quercus frainetto t. (%)
Pistacia (%)
Ulmus (%)
Tilia (%)
Fraxinus angustifolia t. (%)
Corylus (%)
Juniperus stomata
Juniperus t. (%)
Pinus stomata
Pinus nigra/sylvestris t. (%)
Abies (%)
Carpinus betulus (%)
Ostrya carpinifolia t. (%)
Fagus (%)
(j) Pollen zones
VEG-1
VEG-2
VEG-3
VEG 4
VEG-5
VEG-6
VEG 7
9000
8000
7000
6000
5000
4000
3000
2000
1000
0
Age (cal. BP)

Figure 5

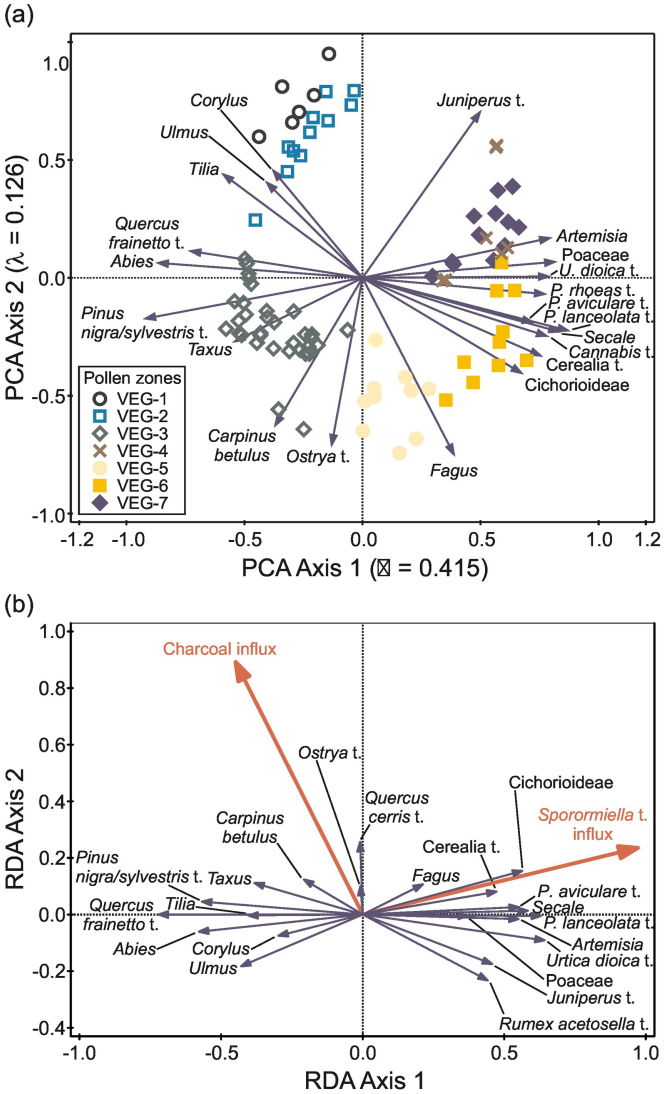
(a)
PCA Axis 2 (λ = 0.126)
PCA Axis 1 (λ = 0.415)
Corylus
Ulmus
Tilia
Quercus frainetto t.
Abies
Pinus nigra/sylvestris t.
Taxus
Carpinus betulus
Ostrya t.
Fagus
Juniperus t.
Artemisia
Poaceae
U. dioica t.
P. rhoeas t.
P. aviculare t.
P. lanceolata t.
Secale
Cannabis t.
Cerealia t.
Cichorioideae
Pollen zones
VEG-1
VEG-2
VEG-3
VEG-4
VEG-5
VEG-6
VEG-7
(b)
RDA Axis 2
RDA Axis 1
Charcoal influx
Ostrya t.
Quercus cerris t.
Cichorioideae
Sporormiella t. influx
Carpinus betulus
Cerealia t.
Pinus nigra/sylvestris t.
Taxus
Fagus
Quercus frainetto t.
Tilia
P. aviculare t.
Secale
P. lanceolata t.
Abies
Corylus
Ulmus
Artemisia
Urtica dioica t.
Poaceae
Juniperus t.
Rumex acetosella t.

Figure 6